
Detailed Studies of Electron Cooling Friction Force

Alexei Fedotov

(September 30, 2005)

Outline

2

Part 1:

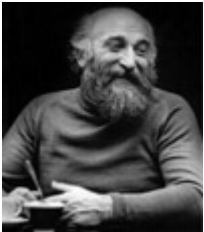
Numerical studies and comparison with theory.

A. Fedotov, D. Bruhwiler, D. Abell, A. Sidorin, "Detailed studies of the friction force", COOL05 Workshop (Galena, IL)

Part 2:

Experimental studies of the friction force.

A. Fedotov, B. Galnander, V. Litvinenko, T. Lofnes, A. Sidorin, A. Smirnov, V. Ziemann, "Experimental benchmarking of the magnetized friction force", COOL05 Workshop (Galena, IL)

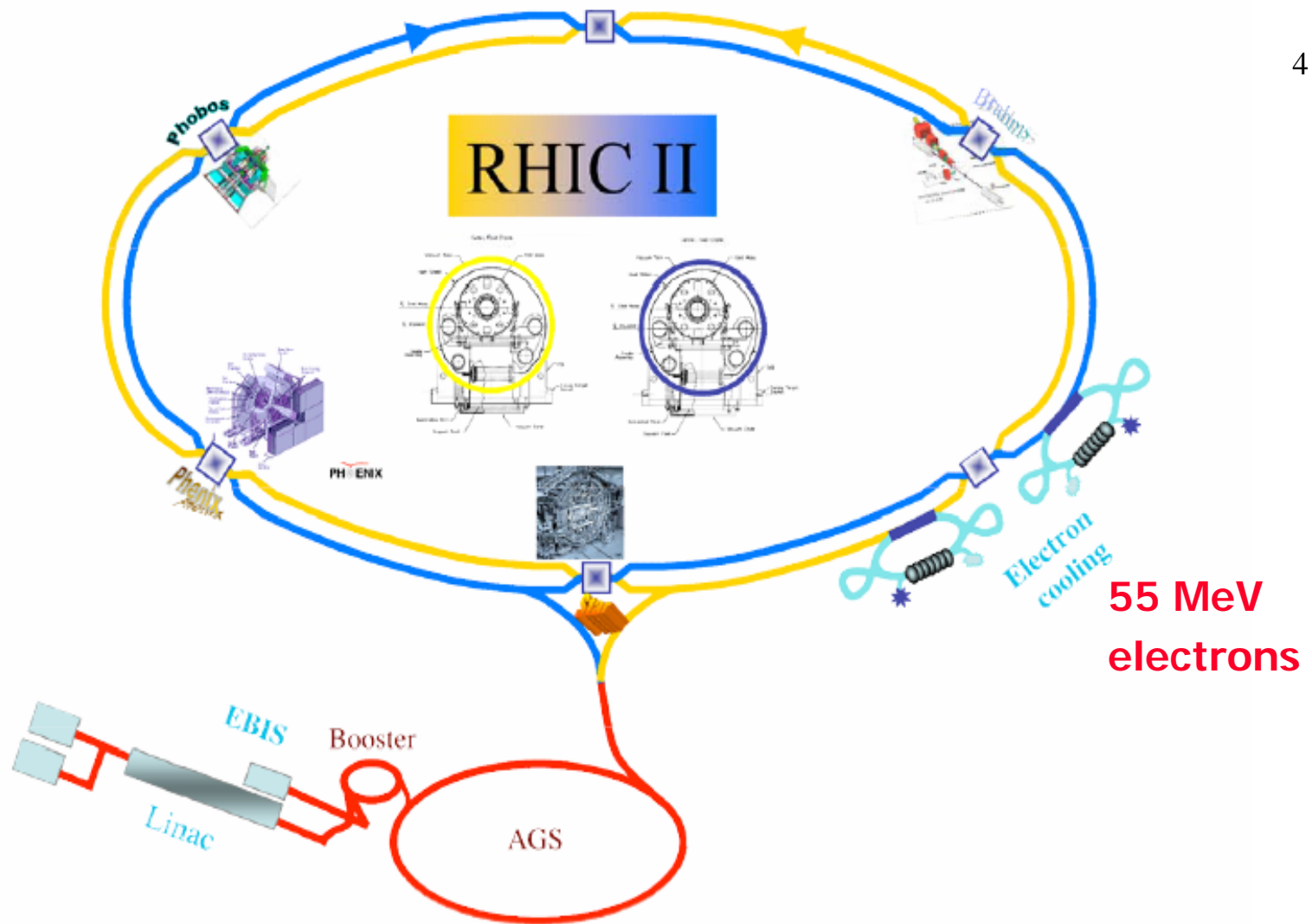


Electron cooling
was invented by
G.I. Budker
(INP, Novosibirsk, 1966)



First experimental
cooling. NAP-M storage
ring (Novosibirsk, 1974)

1. Low-energy (3-300 KeV electrons) cooling (1974-2005): 10's of coolers were constructed and successfully operated – **all based on magnetized cooling.**
2. Medium-energy (4 MeV) cooling at FNAL: **first non-magnetized cooling demonstrated July 2005.**
3. Future medium and high-energy cooling projects: HESR (GSI) and RHIC-II (BNL).



Practical implementation of e-cooling

5

1. Produce a beam of cold (low emittance) electrons.
2. Move these electrons with a velocity of the heavy particles to be cooled.
3. Heavy particles scatter off the electrons and energy is transferred to electrons. This energy transfer appears as a friction force acting on the ions. The ions are “cooled”.
4. The electrons are renewed.

Physics of magnetized and non-magnetized cooling

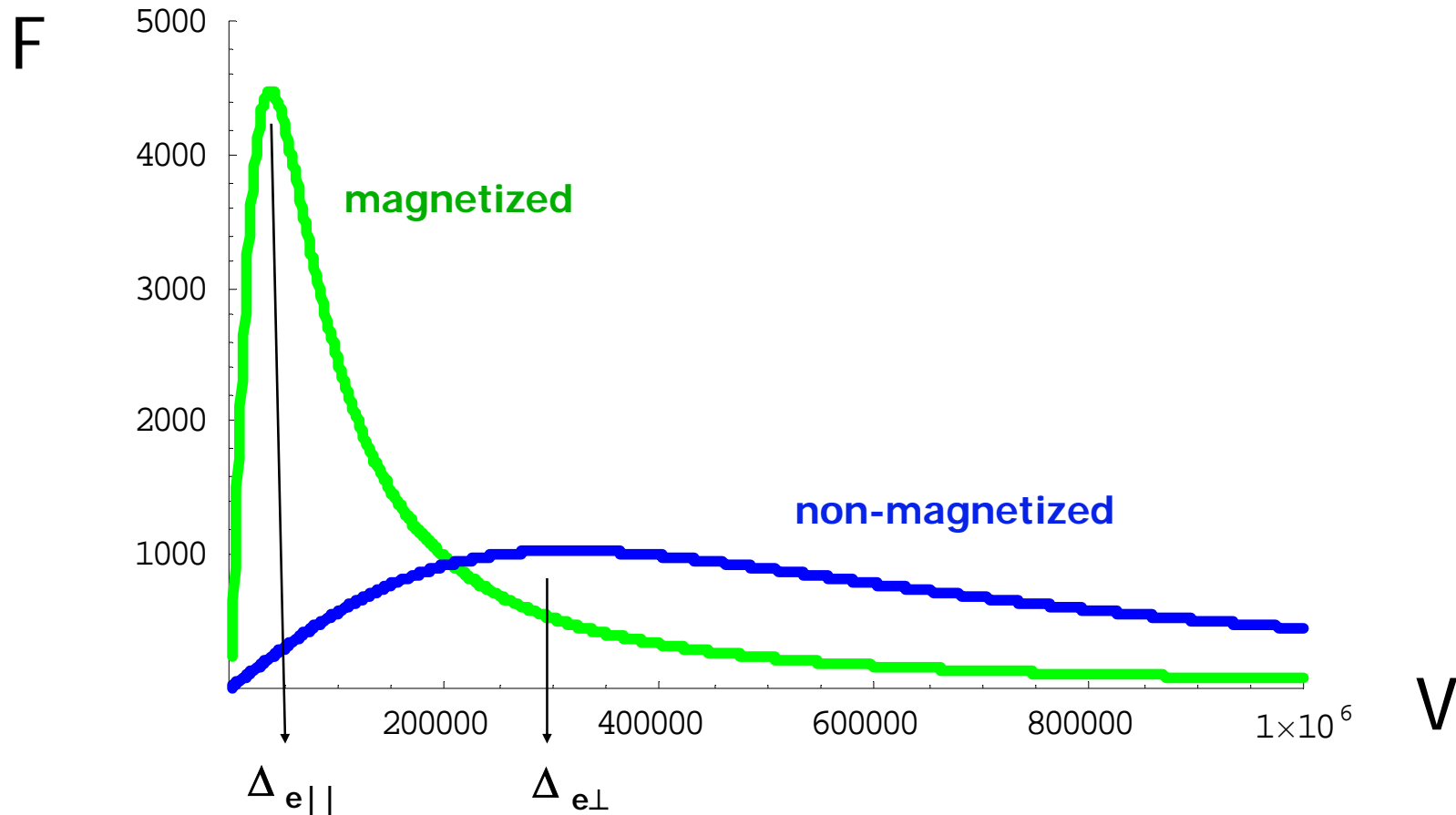
6

1. **Non-magnetized cooling:** thermal velocity of electrons smaller than the velocity spread of ions which needs to be cooled.
2. **Magnetized cooling:** strong magnetic field limits transverse motion of electrons, so that transverse degree of freedom does not take part in the energy exchange. As a result, the efficiency of cooling is determined only by the longitudinal velocity spread of electrons.

In typical low-energy coolers longitudinal velocity spread of electrons is much smaller than transverse – **strong velocity anisotropy together with magnetic field leads to “fast cooling”**.

Schematic friction force for magnetized and non-magnetized cooling

7



Future high-energy coolers

8

1. HESR (GSI) cooler – up to 8MeV electrons. Present baseline 4MeV as in FNAL. However, it needs to be magnetized cooling – many technical issues.
2. RHIC-II (BNL)– cooling with bunched electron beam with energy up to 55MeV - first high-energy cooling based on new technology.

Limitation of magnetized cooling at high-energy₉

A problem of Magnetized Cooling for high-energy is that “**effective longitudinal spread of electron**” due to magnetic imperfection can be rather big:

1. RHIC (BNL): $\gamma=100$, $\theta=1e-5$, $\theta_{\text{effective}}=\gamma\theta=1e-3$

To get significant advantage from “good Magnetized Cooling” – one needs to make precise solenoid (or have a scheme of precise alignment). The main purpose of magnetized cooling approach for RHIC is to kill recombination.

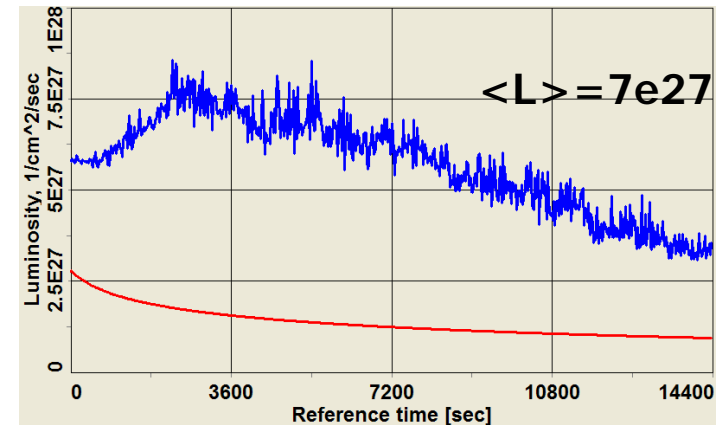
2. HESR (GSI): $\gamma=9$, $\theta=1e-5$, $\theta_{\text{effective}}=9e-5$

RHIC e-cooling

10

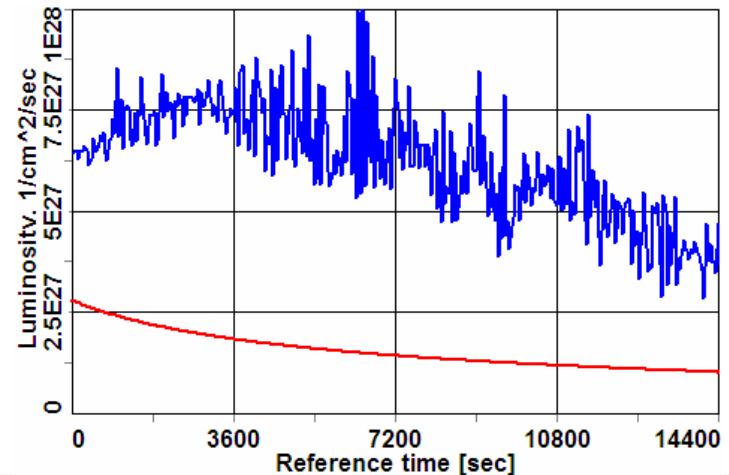
For electron cooling in RHIC (Au ions at $\gamma=108$) we studied two approaches:

1. **Magnetized cooling** - $B=2\text{-}5\text{T}$ solenoid, $L=2\times 30\text{m}$, $q=20\text{nC}$, $\epsilon_e=50\text{um}$



Factor of 10 increase in luminosity in both approaches

2. **Non-magnetized cooling** (with helical wigglers to control recombination) - $B=20\text{-}50\text{G}$, $L=2\times 30\text{m}$, $q=2\text{-}5\text{nC}$, $\epsilon_e=2\text{-}3\text{um}$



RHIC E-cooler Design Report
<http://www.agsrhichome.bnl.gov/eCool>

High-energy cooling: need for accurate predictions of cooling times

11

Cooling times for relativistic energies are much longer than for typical coolers:

$$\tau = \frac{A}{Z^2} \frac{\gamma^2}{4\pi r_p r_e n_e c \eta \Lambda_c} \left(\frac{\gamma \mathcal{E}_{in}}{\beta_{ic}} \right)^{3/2}$$

- standard (order of magnitude) estimate of cooling times for Au ion at RHIC storage energy of 100 GeV gives τ of the order of **1000 sec**, compared to a typical cooling time of the order of **0.1-1 sec** in existing coolers
- while an order of magnitude estimate was sufficient for typical coolers it becomes unacceptable for RHIC with a store time of a few hours and fast emittance degradation due to Intra Beam Scattering (IBS)



We need computer simulations which will give us cooling times estimates with an accuracy much better than an order of magnitude.

Accurate description of the Cooling Force

12

Cooling Force studies



1. Benchmarking of available formulas vs VORPAL code (direct simulation of friction force) for various regimes.

D. Bruhwiler et al., AIP Conf. Proc. 773 (Bensheim, Germany, 2004), p.394.

A. Fedotov et al.; Bruhwiler et al., Proceedings of PAC'05 (Knoxville, TN, 2005).

2. Experimental benchmarking:

(CELSIUS, December 2004 and March 2005)

Part 1

(Friction force formulas: theory and simulations)

A. Fedotov (BNL), D. Bruhwiler, D. Abell (Tech-X), A. Sidorin (JINR)

Comparison with theory

14

At a minimum, we want to be sure that we are using the most appropriate and accurate cooling force formulas.

Magnetized friction force:

“electron cooling theory is well understood”

1. Infinite magnetic field approximation (Derbenev-Skrinsky (D-S), Derbenev-Skrinsky-Meshkov (D-S-M)).
2. Empiric formula (V. Parkhomchuk (VP)) (any strength of the field) – can show very different cooling dynamics for some parameters. Also, has different numerical factors.

Different formulas agree with one another within factor of 3-10 , depending on the parameters – not good for high-energy estimates.

Non-magnetized force:

More straightforward – but one needs to use correct expressions - we did comparison of typically used asymptotic formulas and direct numerical integration.

Codes used for Friction Force studies

15

We use:

1. VORPAL code – uses molecular dynamics techniques to explicitly resolve close binary collisions and thus capture friction and diffusion tensors with a bare minimum of physical assumptions.

C. Nieter, J. Cary, J. Comp. Phys. 196, p. 448 (2004)

D. Bruhwiler et al., AIP Conf. Proc. 773 (Bensheim, 2004), p. 394.

2. Numerical integration of analytic formulas over electron velocity distribution and comparison with simple asymptotic expressions using BETACOOOL code

The BETACOOOL program, <http://lepta.jinr.ru>

Non-magnetized friction force (B=0) – isotropic electron distribution

16

$$\vec{F} = -\frac{4\pi n_e e^4 Z^2 L}{m} \int \frac{\vec{v}_i - \vec{v}_e}{|\vec{v}_i - \vec{v}_e|^3} f(v_e) d^3 v_e$$

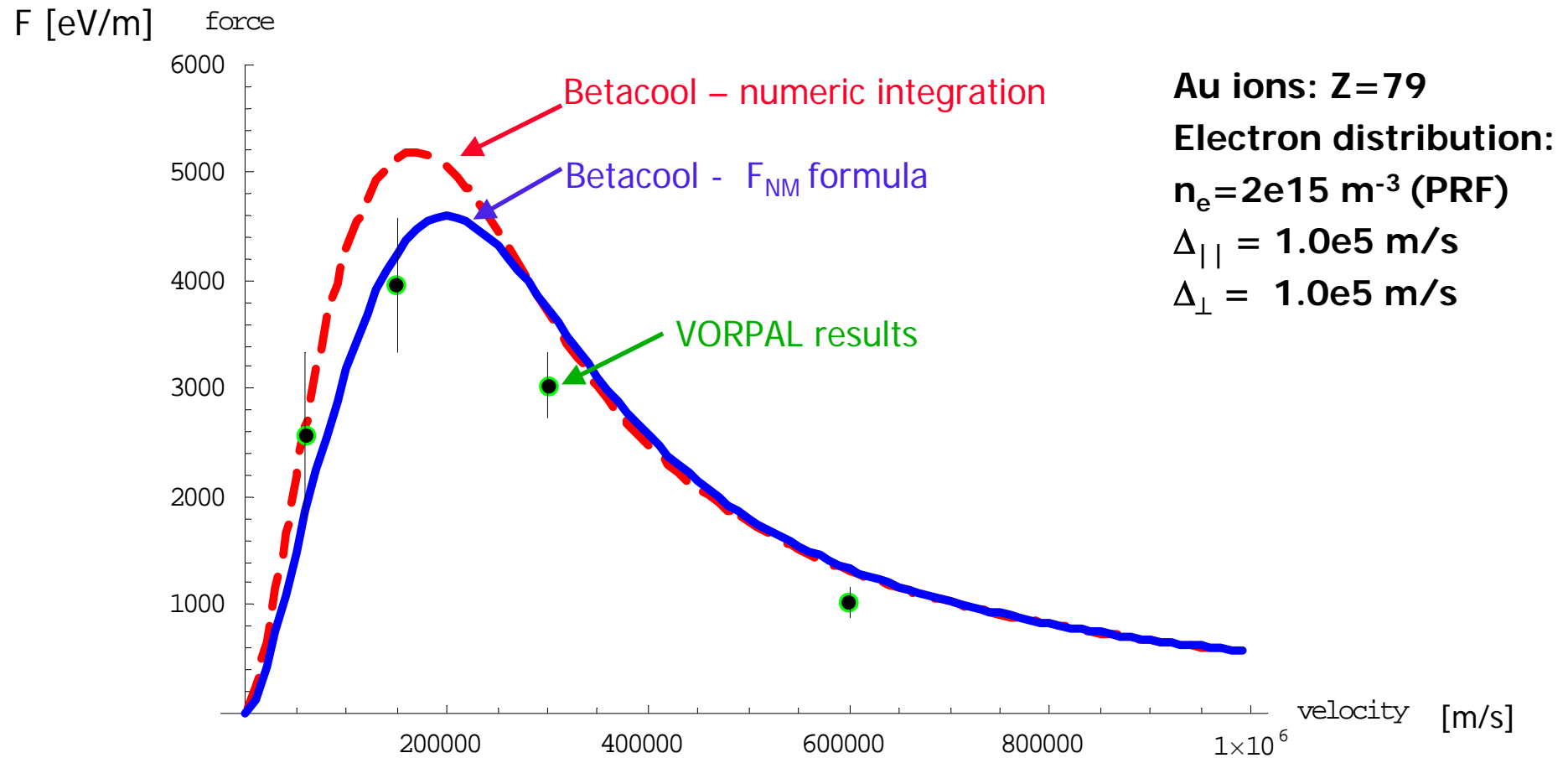
For isotropic Maxwellian distribution $f(v_e)$ (Chandrasekar 1942):

$$\vec{F}_{NM}(\vec{v}_i) = -\frac{\vec{v}_i}{v_i^3} \frac{4\pi n_e e^4 Z^2 L}{m} \varphi\left(\frac{v_i}{\Delta_e}\right)$$

$$\varphi(x) = \sqrt{\frac{2}{\pi}} \int_0^x e^{-y^2/2} dy - \sqrt{\frac{2}{\pi}} x e^{-x^2/2}$$

B=0, isotropic electron distribution for ion velocity along the longitudinal direction

17



B=0 – anisotropic electron velocity distribution (typical situation for electron coolers)

18

Numerical evaluation (BETACOOOL):

$$F_{\perp} = -\frac{4\pi Z^2 e^4 n_e}{m \cdot \text{Int}} \int_0^{3\Delta_{\perp}} \int_{-3\Delta_{\parallel}}^{3\Delta_{\parallel}} \int_0^{\pi} \ln\left(\frac{\rho_{\max}}{\rho_{\min}}\right) \frac{(V_{\perp} - v_{\perp} \cos \varphi) \exp\left(-\frac{v_{\perp}^2}{2\Delta_{\perp}^2} - \frac{v_{\parallel}^2}{2\Delta_{\parallel}^2}\right)}{\left((V_{\parallel} - v_{\parallel})^2 + (V_{\perp} - v_{\perp} \cos \varphi)^2 + v_{\perp}^2 \sin^2 \varphi\right)^{3/2}} v_{\perp} d\varphi dv_{\parallel} dv_{\perp}$$

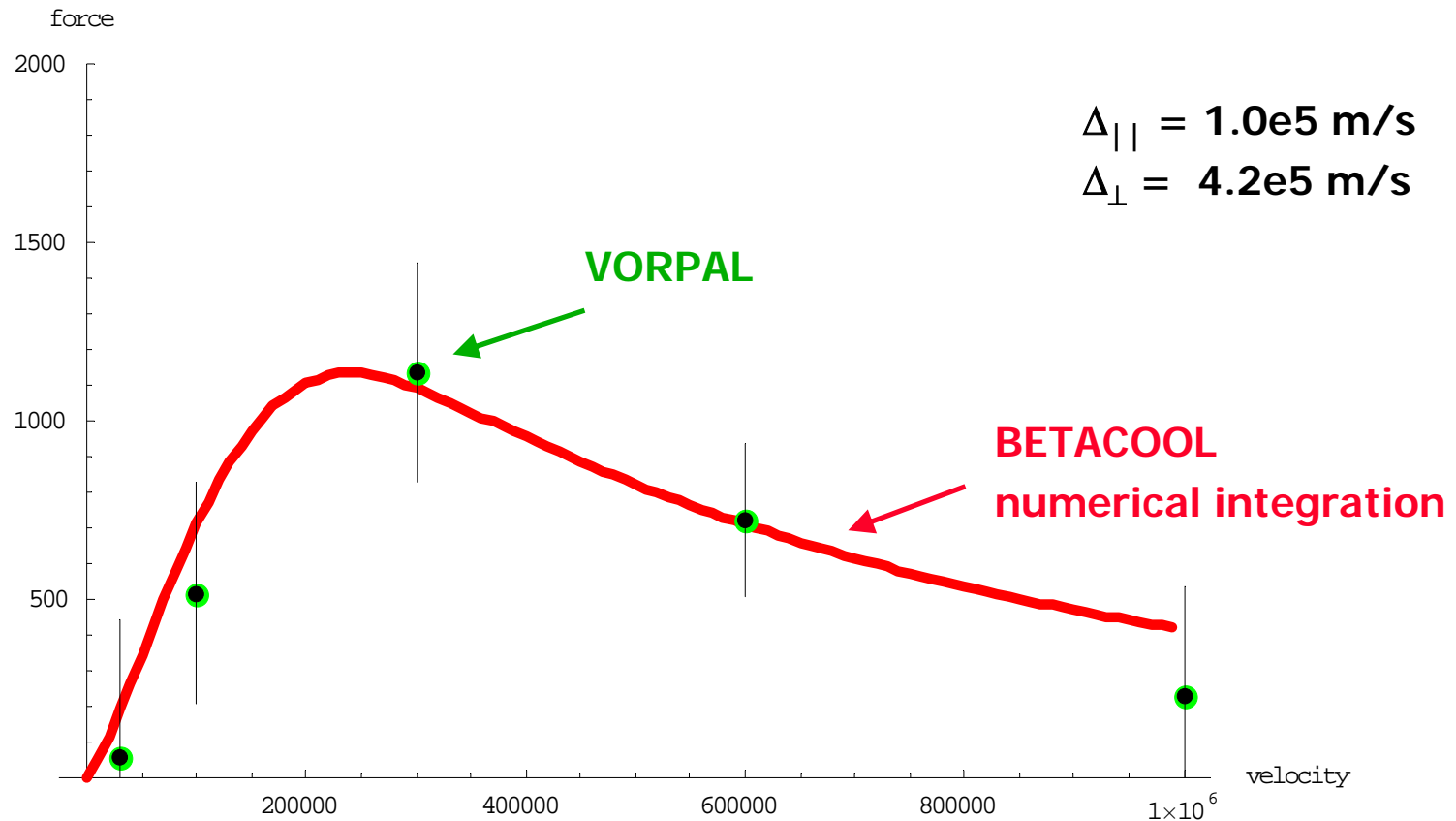
$$F_{\parallel} = -\frac{4\pi Z^2 e^4 n_e}{m \cdot \text{Int}} \int_0^{3\Delta_{\perp}} \int_{-3\Delta_{\parallel}}^{3\Delta_{\parallel}} \int_0^{\pi} \ln\left(\frac{\rho_{\max}}{\rho_{\min}}\right) \frac{(V_{\parallel} - v_{\parallel}) \exp\left(-\frac{v_{\perp}^2}{2\Delta_{\perp}^2} - \frac{v_{\parallel}^2}{2\Delta_{\parallel}^2}\right)}{\left((V_{\parallel} - v_{\parallel})^2 + (V_{\perp} - v_{\perp} \cos \varphi)^2 + v_{\perp}^2 \sin^2 \varphi\right)^{3/2}} v_{\perp} d\varphi dv_{\parallel} dv_{\perp}$$

Asymptotic formulas – can significantly overestimate friction force, especially near the longitudinal rms velocity spread

$$\begin{aligned} & (v_i \ll \Delta_{\parallel}) \quad F_{\parallel} = -\frac{4\pi Z^2 e^4 n_e L}{m} \frac{v_{\parallel}}{\Delta_{\parallel} \Delta_{\perp}^2} \\ & (\Delta_{\parallel} \ll v_i \ll \Delta_{\perp}) \quad \vec{F}_{\perp} = -\frac{4\pi Z^2 e^4 n_e L}{m} \frac{v_{i,\perp}}{\Delta_{\perp}^3} \quad F_{\parallel} = -\frac{4\pi Z^2 e^4 n_e L}{m} \frac{v_{\parallel}}{|v_{\parallel}| \Delta_{\perp}^2} \\ & (v_i \gg \Delta_{\perp}) \quad \vec{F} = -\frac{4\pi Z^2 e^4 n_e L}{m} \cdot \frac{\vec{v}_i}{v^3} \end{aligned}$$

B=0, anisotropic velocity distribution

19



Non-magnetized force - summary

20

For anisotropic velocity distribution:

1. VORPAL gives good agreement with numerical integrals.
2. Asymptotic formulas overestimate friction force by a significant factor for typical RHIC parameters.

We are presently using numerical integrals in BETACOOOL in our cooling dynamics studies for the non-magnetized cooling.

Magnetized friction force

- approximation of strong magnetic field

21

Numerical integration using Derbenev-Skrinsky (D-S) expressions for the magnetized collisions (BETACOOl):

$$F_{\perp}(V_{\perp}, V_{\parallel}) = -\frac{2\pi Z^2 e^4 n_e L_M}{m} \int \frac{V_{\perp} (V_{\perp}^2 - 2(V_{\parallel} - v_e)^2)}{(V_{\perp}^2 + (V_{\parallel} - v_e)^2)^{5/2}} f(v_e) dv_e$$

$$F_{\parallel}(V_{\perp}, V_{\parallel}) = -\frac{2\pi Z^2 e^4 n_e}{m} \int \left(L_M \frac{3V_{\perp}^2 (V_{\parallel} - v_e)}{(V_{\perp}^2 + (V_{\parallel} - v_e)^2)^{5/2}} + 2 \frac{V_{\parallel} - v_e}{(V_{\perp}^2 + (V_{\parallel} - v_e)^2)^{3/2}} \right) f(v_e) dv_e$$

Asymptotic expressions for all three type of collisions
(Derbenev-Skrinsky-Meshkov (D-S-M)):

$$F_{\perp} \approx -\frac{2\pi Z^2 e^4 n_e}{m} v_{\perp} \left\{ \begin{array}{l} \frac{1}{v^3} \left(2L_F + \frac{v_{\perp}^2 - 2v_{\parallel}^2}{v^2} L_M \right), \{I\} \\ \frac{2}{\Delta_{\perp}^3} (L_F + N_{col} L_A) + \frac{v_{\perp}^2 - 2v_{\parallel}^2}{v^2} \frac{L_M}{v^3}, \{II\} \\ \frac{2}{\Delta_{\perp}^3} (L_F + N_{col} L_A) + \frac{L_M}{\Delta_{\parallel}^3}, \{III\} \end{array} \right. \quad F_{\parallel} \approx -\frac{2\pi Z^2 e^4 n_e}{m} v_{\parallel} \left\{ \begin{array}{l} \frac{1}{v^3} \left(2L_F + \frac{3v_{\perp}^2}{v^2} L_M + 2 \right), \{I\} \\ \frac{2}{\Delta_{\perp}^2 v_{\parallel}} (L_F + N_{col} L_A) + \left(\frac{3v_{\perp}^2}{v^2} L_M + 2 \right) \frac{1}{v^3}, \{II_a\} \\ \frac{2}{\Delta_{\perp}^2 \Delta_{\parallel}} (L_F + N_{col} L_A) + \frac{L_M}{\Delta_{\parallel}^3}, \{II_b, III\} \end{array} \right.$$

Finite magnetic field

22

Empiric formula by V. Parkhomchuk (VP) (NIM, 2000):

$$\vec{F} = -\vec{v} \frac{4Z^2 e^4 n_e L_P}{m} \frac{1}{\left(v^2 + \Delta_{e,eff}^2\right)^{3/2}} \quad L_P = \ln \left(\frac{\rho_{\max} + \rho_{\min} + \langle \rho_{\perp} \rangle}{\rho_{\min} + \langle \rho_{\perp} \rangle} \right)$$

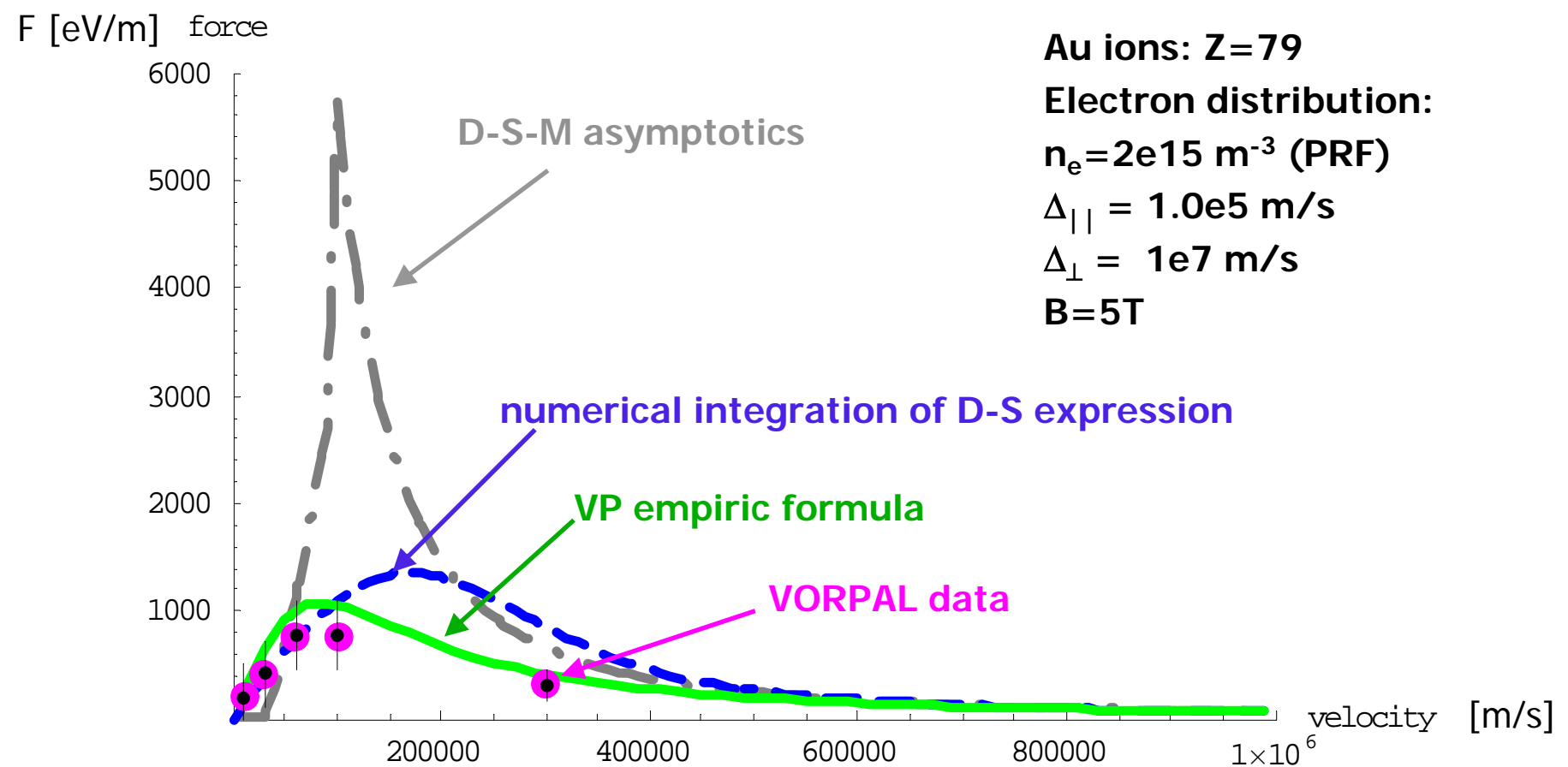
1. Similar to D-S asymptotics at low velocities $v < \Delta_{||}$
2. Very different at large velocities $v \gg \Delta_{||}$ - both in numerical factor and dependence on angle with respect to the magnetic field direction.

Studies were done to explore magnetized friction force formulas in various regimes. Some of these studies are reported in the next few slides, using parameters of the RHIC-II cooler based on the magnetized approach.

Friction force for ion velocity along magnetic field line

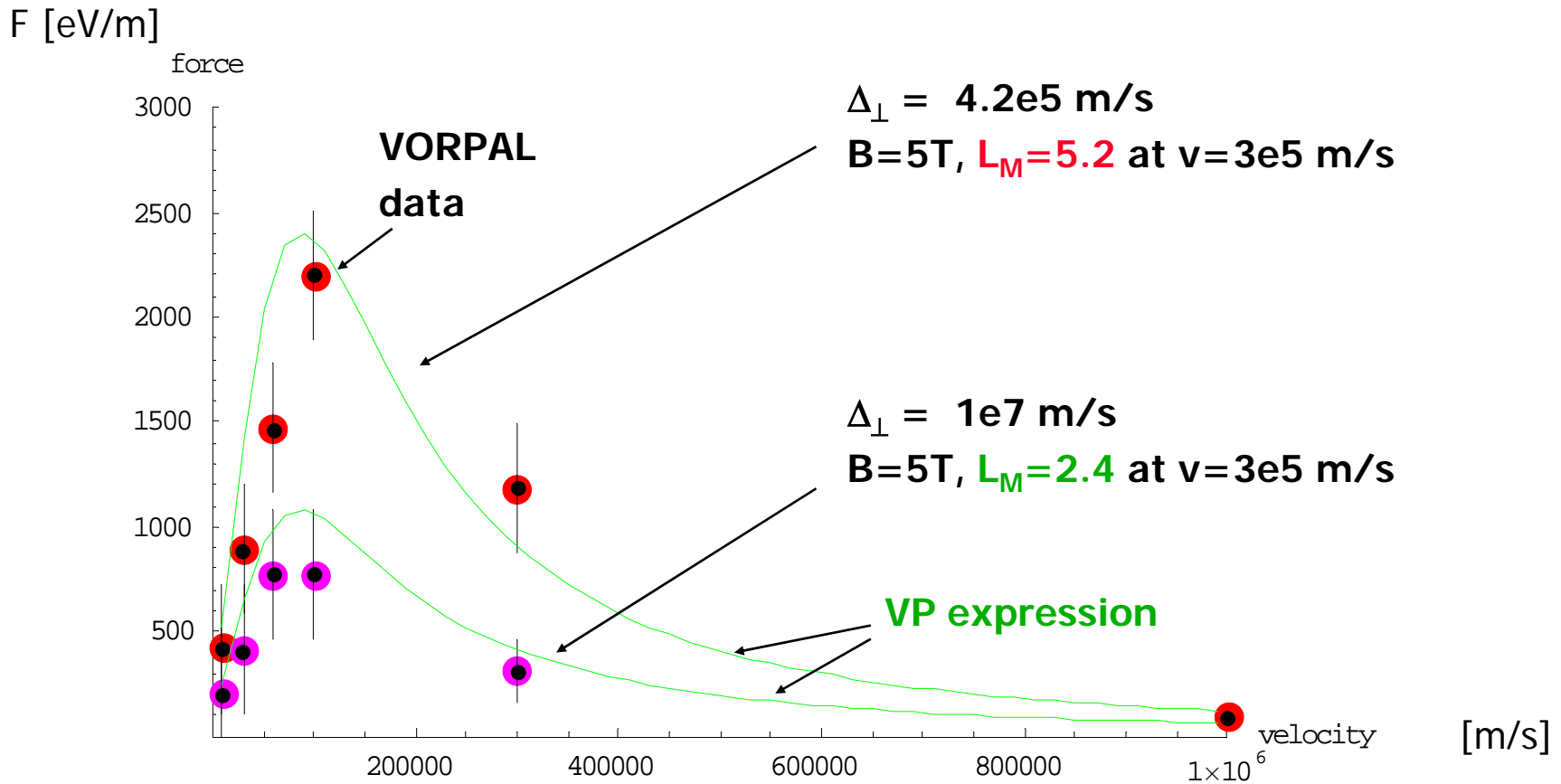
$V_{\perp} = 0$

23



Friction force for ion velocity along magnetic field line ($V_{\perp}=0$) for two different degrees of magnetization

24



Angular dependence at large relative velocities

25

Strong magnetic field results in friction force dependence on the angle with respect to the direction of magnetic field.

Very different expressions for the transverse and longitudinal components of the friction force both of which now depend on both transverse and longitudinal velocity.

But how important is such “angular anisotropy” of the friction force for finite magnetization?

This question was already addressed by Parkhomchuk (NIM, 2000), using simulations with zero temperature electrons. Here we try to examine this question for finite temperatures of electron beam.

Angular dependence for longitudinal component of the friction force

26

empiric formula by V. Parkhomchuk (VP)

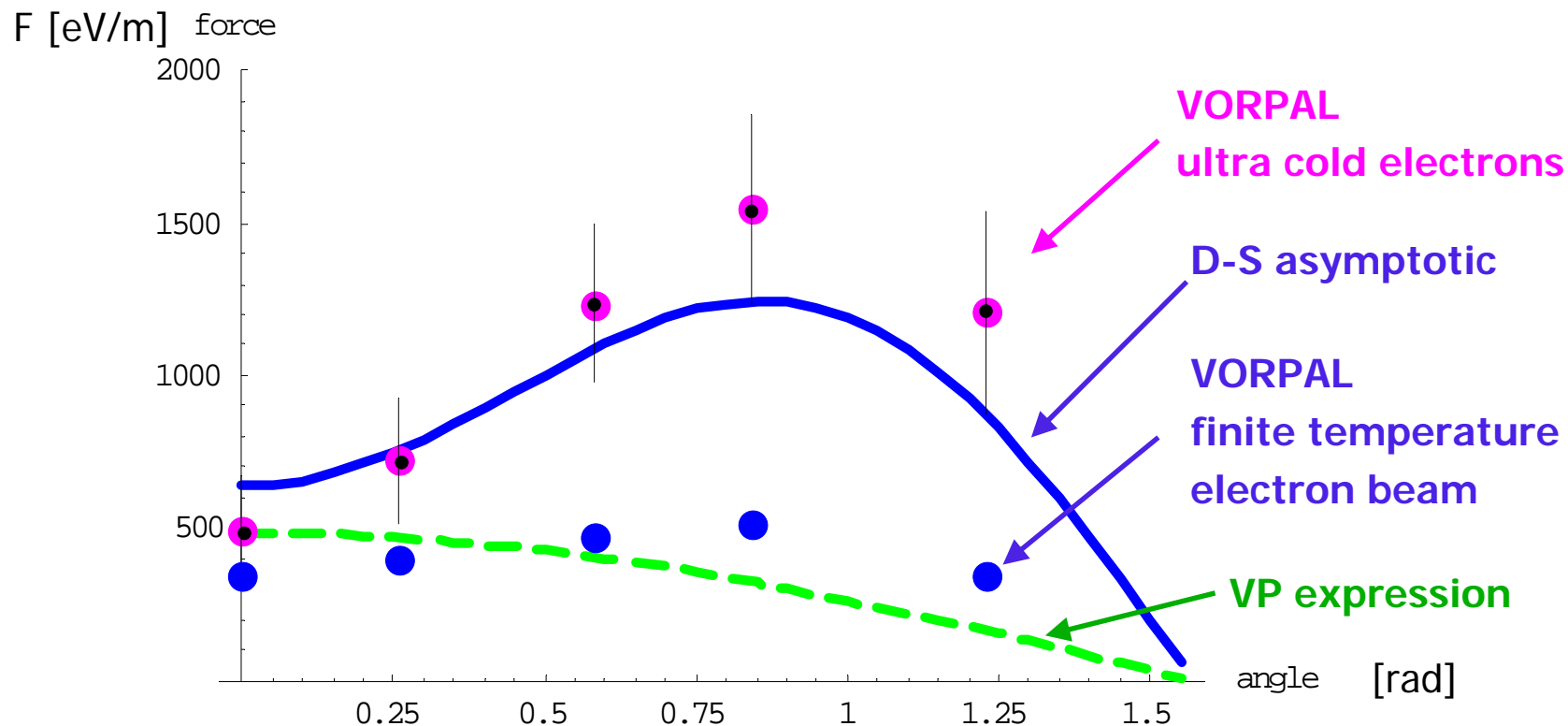
$$\mathbf{F}^{VP} = -\frac{1}{\pi} \omega_{pe}^2 \frac{(Ze)^2}{4\pi\epsilon_0} \Lambda^M \frac{\mathbf{V}_{ion}}{(V_{ion}^2 + V_{eff}^2)^{3/2}}$$

Derbenev-Skrinsky (D-S) asymptotic

$$F_{\parallel}^{DS} = -\frac{3}{2} \omega_{pe}^2 \frac{(Ze)^2}{4\pi\epsilon_0} \left[\Lambda^A(V_{ion}) \left(\frac{V_{\perp}}{V_{ion}} \right)^2 + \frac{2}{3} \right] \frac{V_{\parallel}}{V_{ion}^3}$$

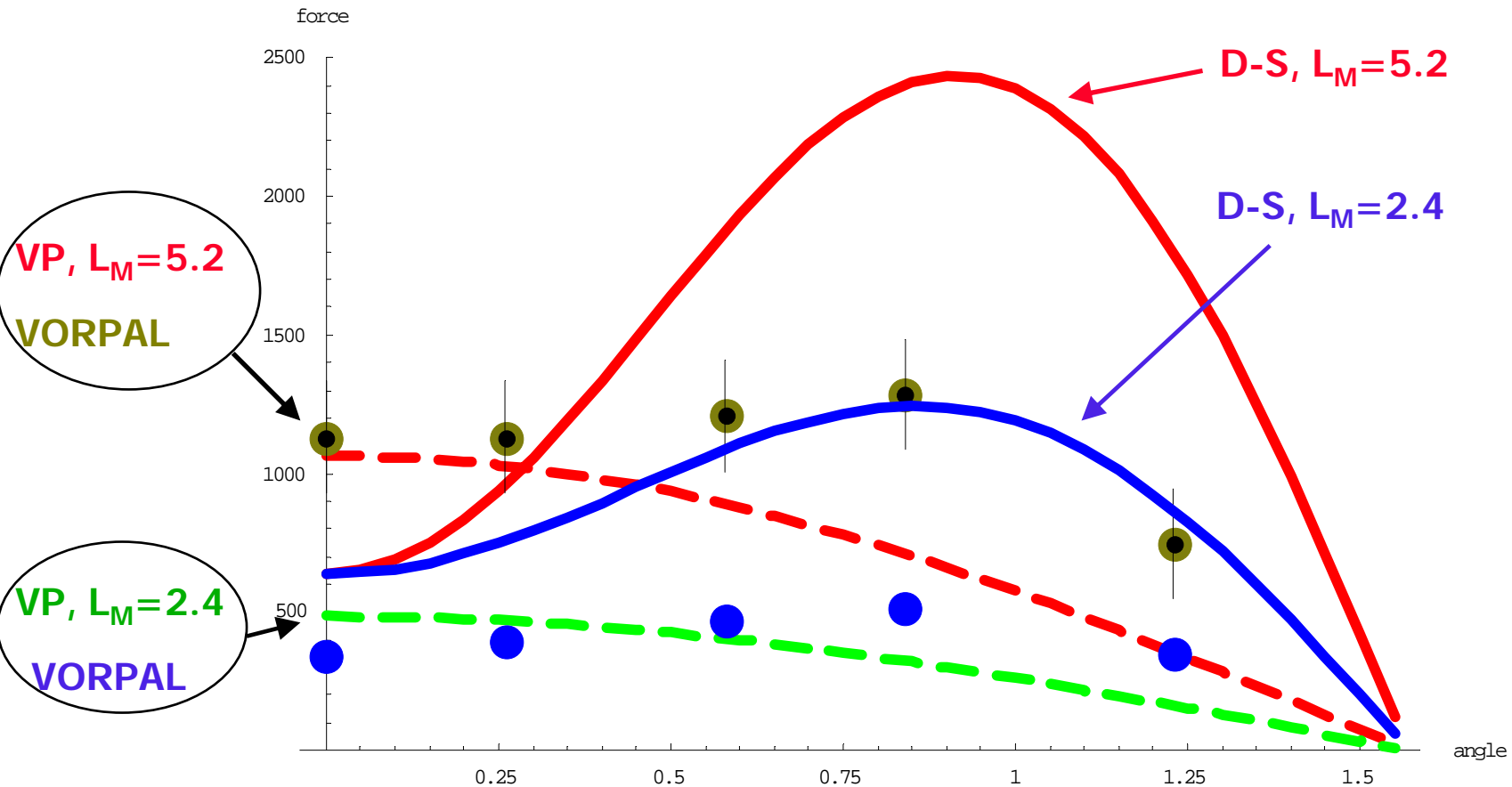
Angular dependence for $V_{ion}=3e5$ m/s ($B=5T$, for $\Delta_{ex,y}=8e6$ m/s, $L_M=2.4$)

27



Longitudinal friction force - scaling with magnetized logarithm for finite temperature electron beam

28



Transverse component of friction force for high velocities $V > \Delta_{e\parallel}$

29

D-S_d (1977)

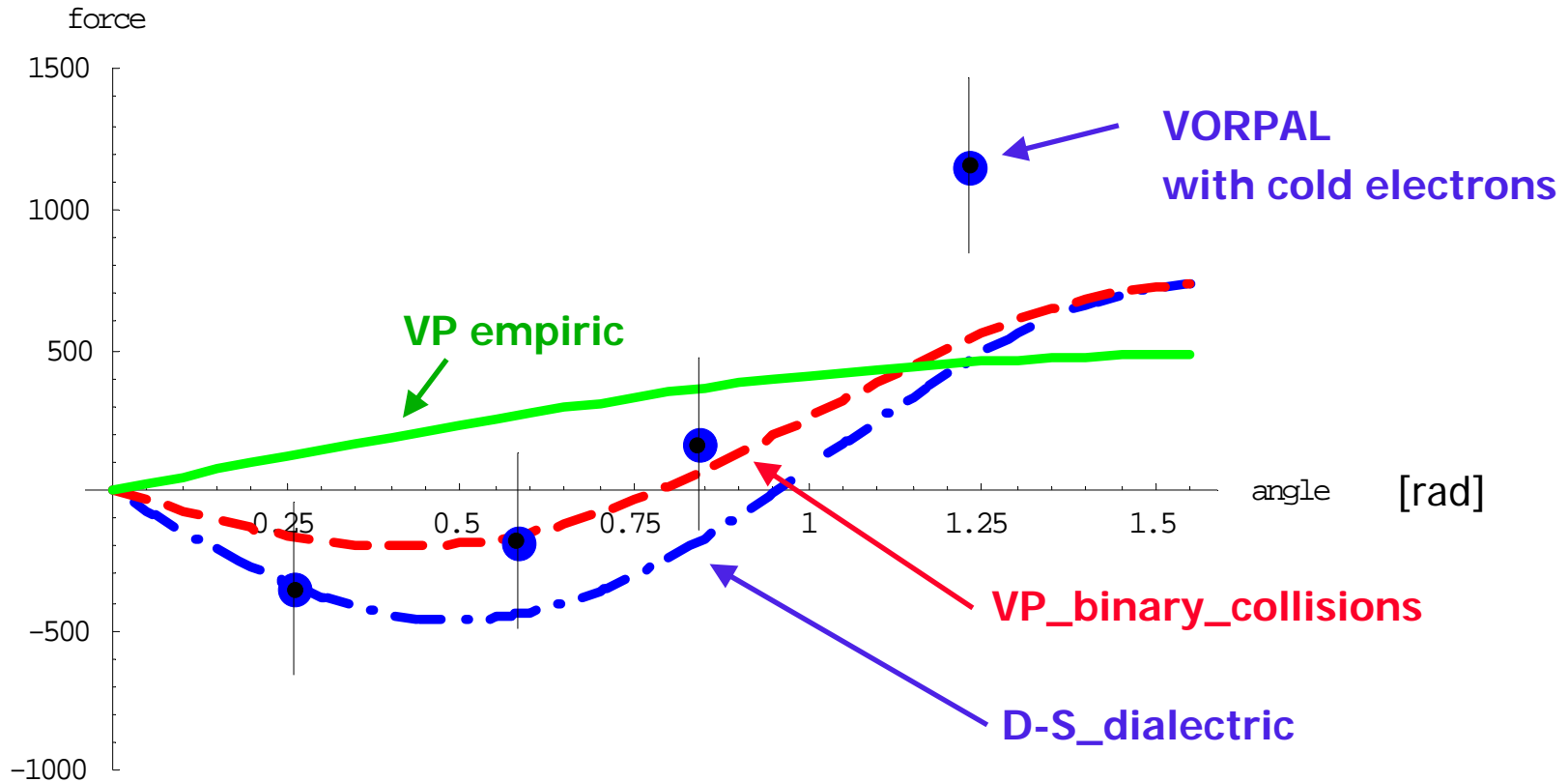
$$F_{\perp, \text{dialectric}}^{DS} = -\frac{1}{2} \omega_{pe}^2 \frac{(Ze)^2}{4\pi\epsilon_0} \Lambda^A(V_{ion}) \frac{(V_{\perp}^2 - 2V_{\parallel}^2)}{V_{ion}^2} \frac{V_{\perp}}{V_{ion}^3}$$

P_{binary collisions} (1984)

$$F_{\perp, \text{binary}}^P = -\frac{1}{2} \omega_{pe}^2 \frac{(Ze)^2}{4\pi\epsilon_0} \Lambda^A(V_{ion}) \frac{(V_{\perp}^2 - V_{\parallel}^2)}{V_{ion}^2} \frac{V_{\perp}}{V_{ion}^3}$$

Angular dependence for the transverse component of the friction force

30



Conclusions on magnetized formulas

31

Using VORPAL code we are now able to explore fine effects in magnetized cooling.

We are studying accuracy of available formulas and theories in various regimes.

Part 2

(Experimental benchmarking of the friction force)

A. Fedotov, V. Litvinenko (BNL)

B. Galnander, T. Lofnes, V. Ziemann (TSL)

A. Sidorin, A. Smirnov (JINR)

Svedberg Laboratory, Uppsala, Sweden (The CELSIUS ring)

33

Team:

Björn Gålnder, Tor Lofnes, Volker Ziemann **TSL, Uppsala, Sweden**

Alexei Fedotov, Vladimir Litvinenko **BNL, USA**

Anatoly Sidorin, Alexander Smirnov **JINR, Dubna, Russia**

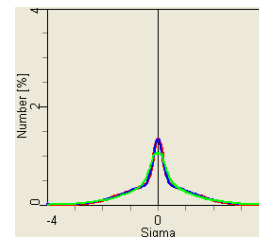
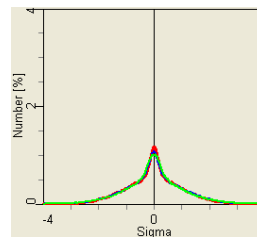
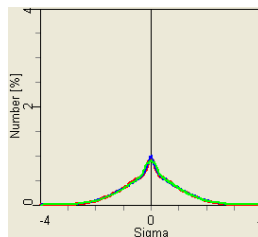


Major goals

34

1. With **well controlled** experiments – systematically study friction force dependence on various parameters such as current, alignment angle, magnetic field.
2. Using low-energy cooler try to reproduce conditions possible at **high-energy cooling**:
 - 2.1) Different magnetization regimes – possible transition from good to bad magnetization
 - 2.2) Transient cooling – when as a result of slow cooling one first has clear formation of beam core with subsequent cooling of tails – need to benchmark IBS models for such distributions.

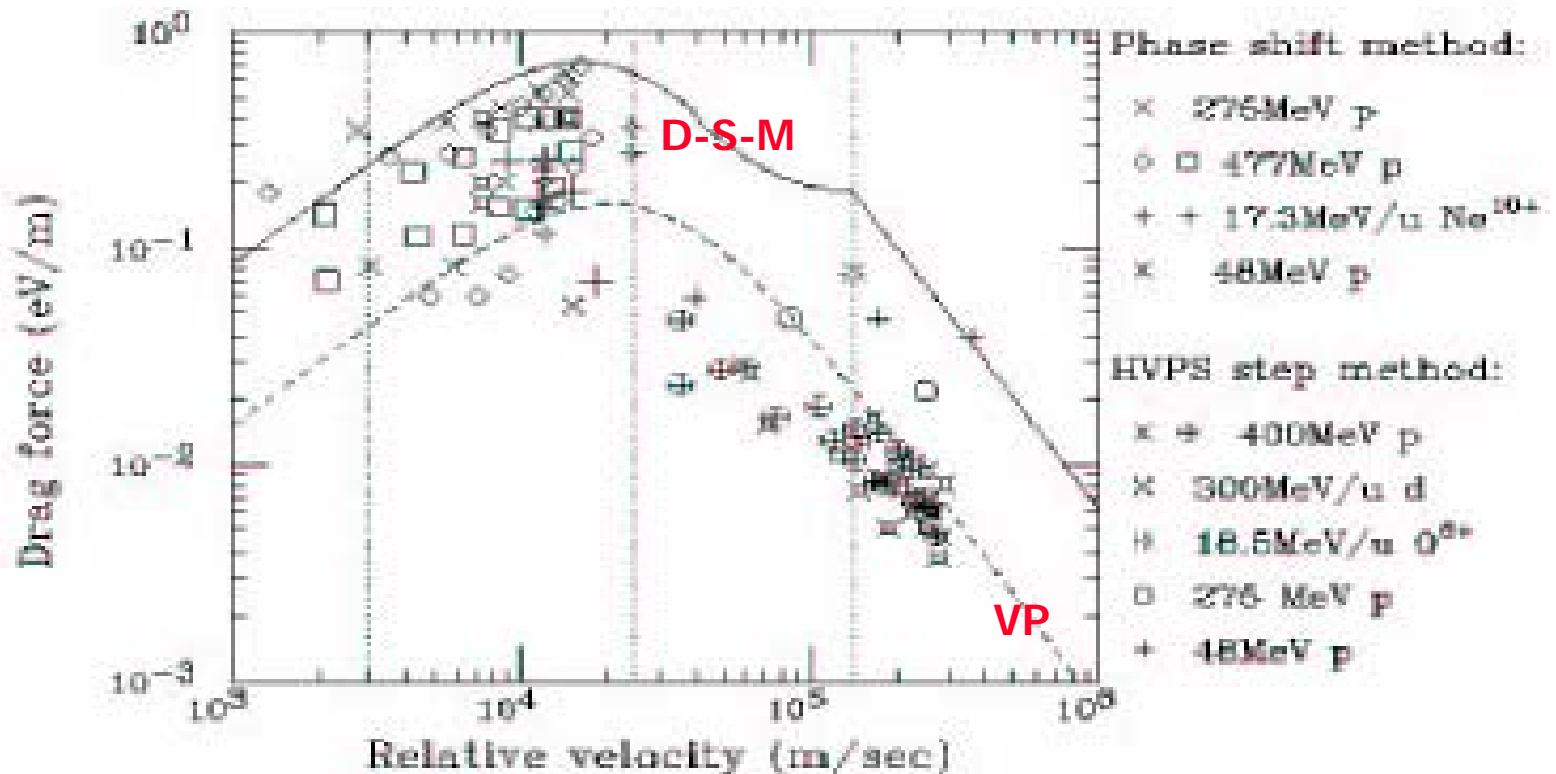
**very important
for collider**



Example of some previous comparison of experimental data with Derbenev-Skrinsky-Meshkov (D-S-M) and V.Parkhomchuk (VP) formulas.

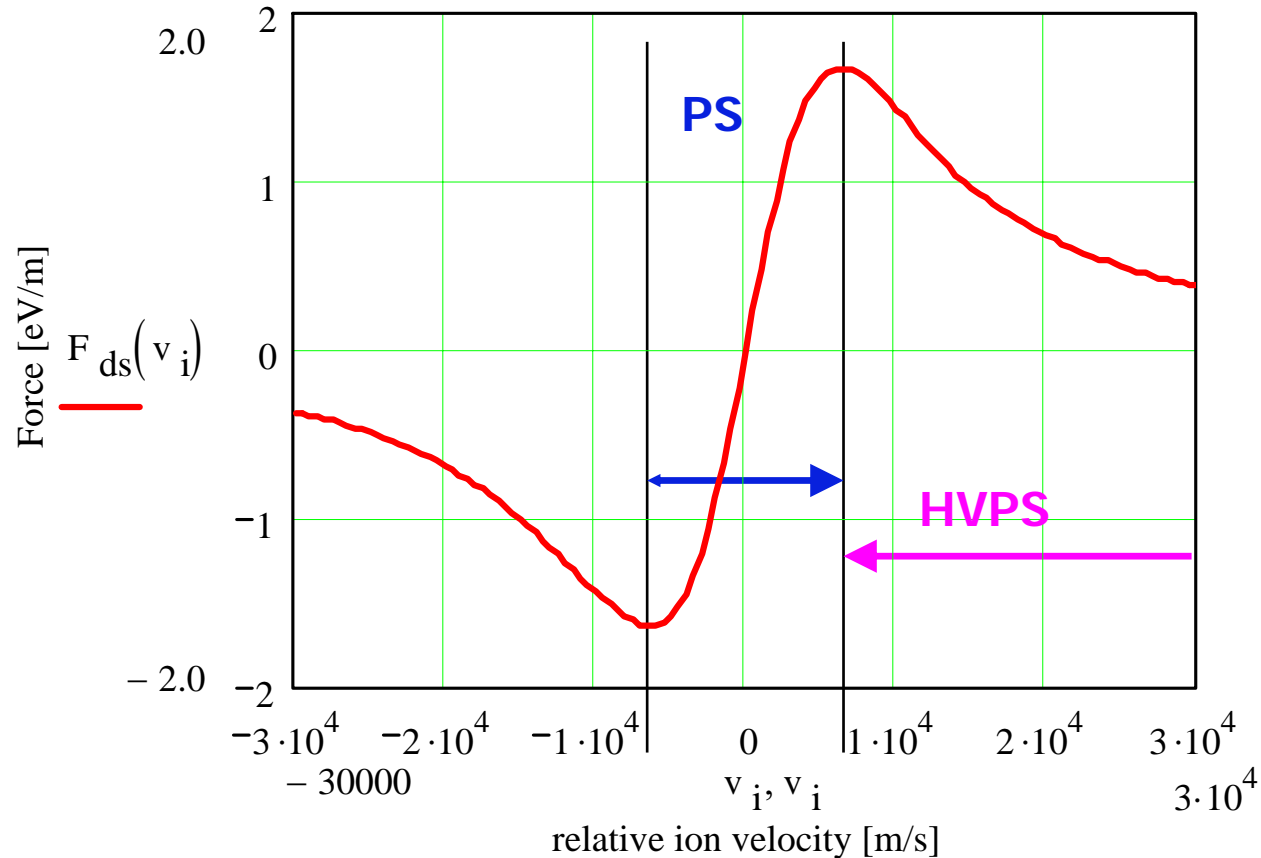
35

Y-N. Rao et al.: CELSIUS, Sweden'2001:



Measurement methods: Phase Shift (PS) and Voltage Step (HVPS)

36



Low relative velocities (linear part and maximum): Phase shift (PS) method

37

- The phase shift method is to apply both the electron cooling and the rf system (bunched ion beam):

measure the phase shift at equilibrium where the energy gain that an ion beam receives on passage through the rf cavity is equal to the energy loss during passage through the cooler

$$F_{\parallel} = \frac{Ze\hat{U}_{rf} \sin \Delta\phi_s}{L_c}$$

U_{rf} –the rf amplitude

$\Delta\phi_s$ –the equilibrium phase difference between the bunch and rf cavity

L_c - length of the cooler

Large relative velocities: HVPS method

38

- The electron beam energy is stepped by quickly changing the HVPS voltage:

The electron beam begins to drag the ion beam as a whole to a new energy corresponding to the new energy of electron beam. During this process the ion beam energy is tracked by recording its Schottky frequency shift

$$F_{\parallel} = \frac{1}{\eta_p} \frac{p_0}{f_0} \frac{\Delta f}{\Delta t} \cdot \frac{1}{\eta_{ec}}$$

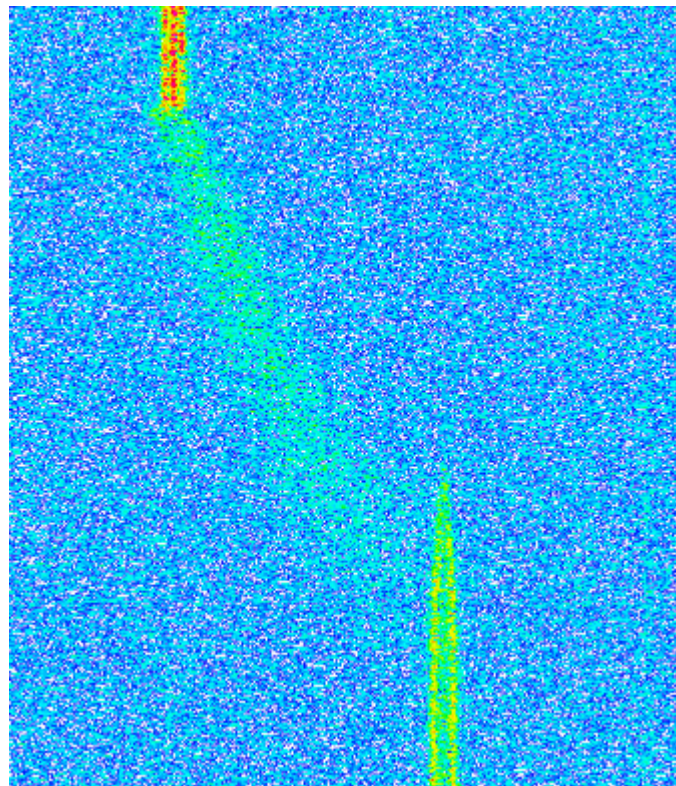
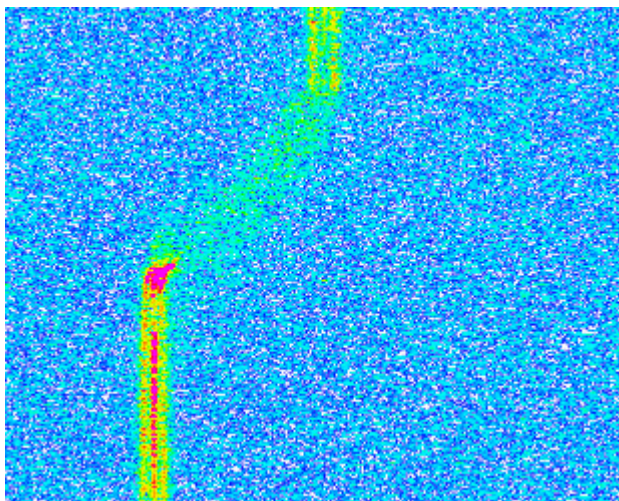
η_p — slippage factor, p_0 is ion momentum

η_{ec} — L/C - ration of cooler length to circumference

Δf - frequency shift recoded during time Δt

Accuracy of HVPS method

39



Accuracy of Phase Shift method: important since it allows us to find exact location of the force maximum

40

1. One needs to introduce small velocity difference between electrons and ions – **typically, voltage step is used to change energy of electrons.**
2. One needs accurate measurement of the phase difference between the bunch and RF signal.

In our experiment at CELSIUS:

1. **Changing RF frequency** – allowed very fine steps in velocity difference (**done before, for example, at IUCF**).
2. Instead of network analyzer without phase lock loop the phase was measured by phase discriminator.

As a result, very accurate experimental data was obtained !

Experiment #1:

41

-
1. $B=0.1\text{T}$, current dependence: ($I_e=500\text{mA}$, 250mA , 100mA , 20 mA)

Measure all needed parameters, including parameters of ion distribution.

Experiment #2:

42

2. Dependence on $V_{\text{effective}}$:

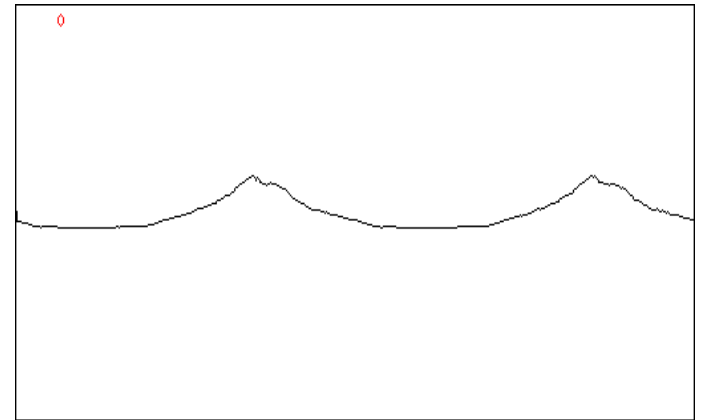
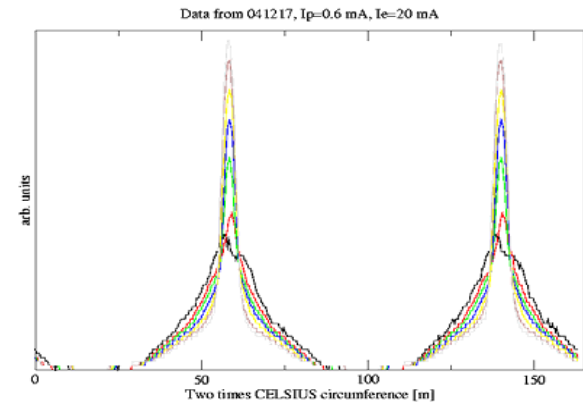
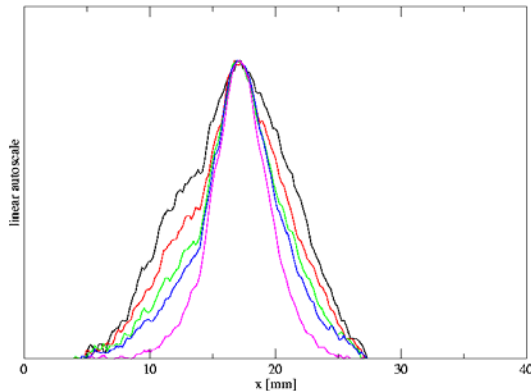
- measured for several values of tilt in both horizontal and vertical direction – both negative and positive directions.
- always recorded longitudinal and transverse sigmas to perform accurate convolution over distributions. Measured values are close to those predicted by BetaCool simulations
- did calibration of tilt angle with both BPM's and H^0 monitor

Experiment #3:

43

3. Measured “transient cooling” (IBS+COOLING) both for longitudinal and transverse profiles:

Test models of IBS for non-Gaussian distribution -needed for high-energy cooling.



Experiment #4:

44

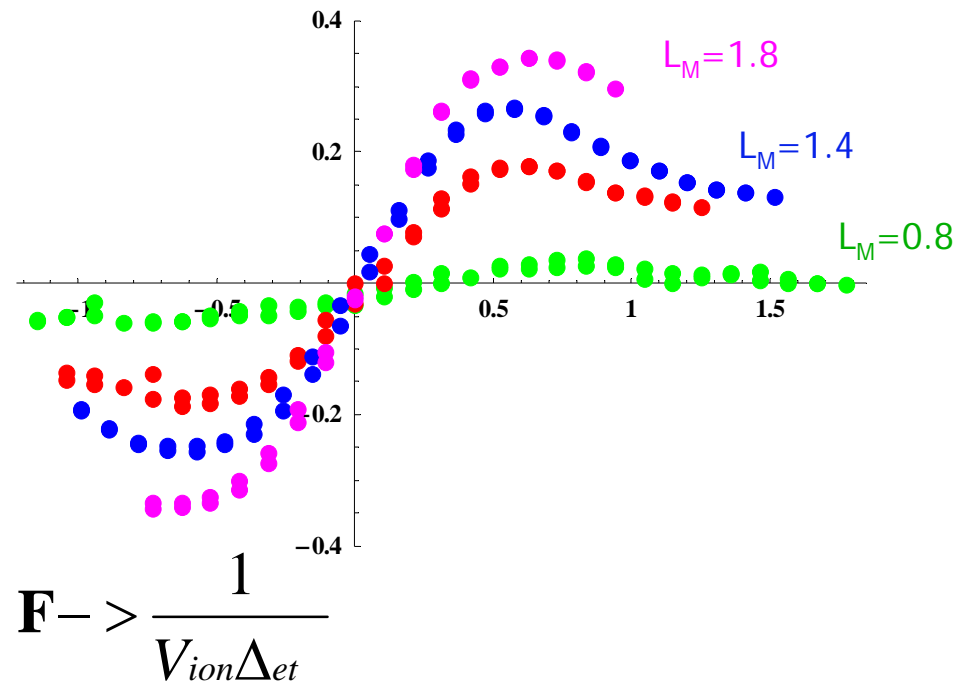
4. Various values of B with various currents: $I_e=500\text{mA}$, 300mA , 100mA , 50mA ($B=0.03, 0.04, 0.05, 0.06, 0.08, 0.1, 0.12\text{T}$) – a lot of careful adjustments for each new setting of magnetic field.

Study various regimes of magnetization – needed for high-energy cooling.

$$L_M = \ln\left(\frac{\rho_{\max}}{r_L} + 1\right) = \frac{\rho_{\max}}{r_L}$$

$$\mathbf{F} = -\frac{1}{\pi} \omega_{pe}^2 \frac{(Ze)^2}{4\pi\epsilon_0} \frac{1}{(V_{ion}^2)} (V\tau eB / m\Delta_{et})$$

$$\mathbf{F} - > \frac{1}{V_{ion}\Delta_{et}}$$



Experiment #5:

45

5. Effects of solenoid errors.

Study description via $V_{\text{effective}}$.

V. Parkhomchuk's (VP) empiric formula

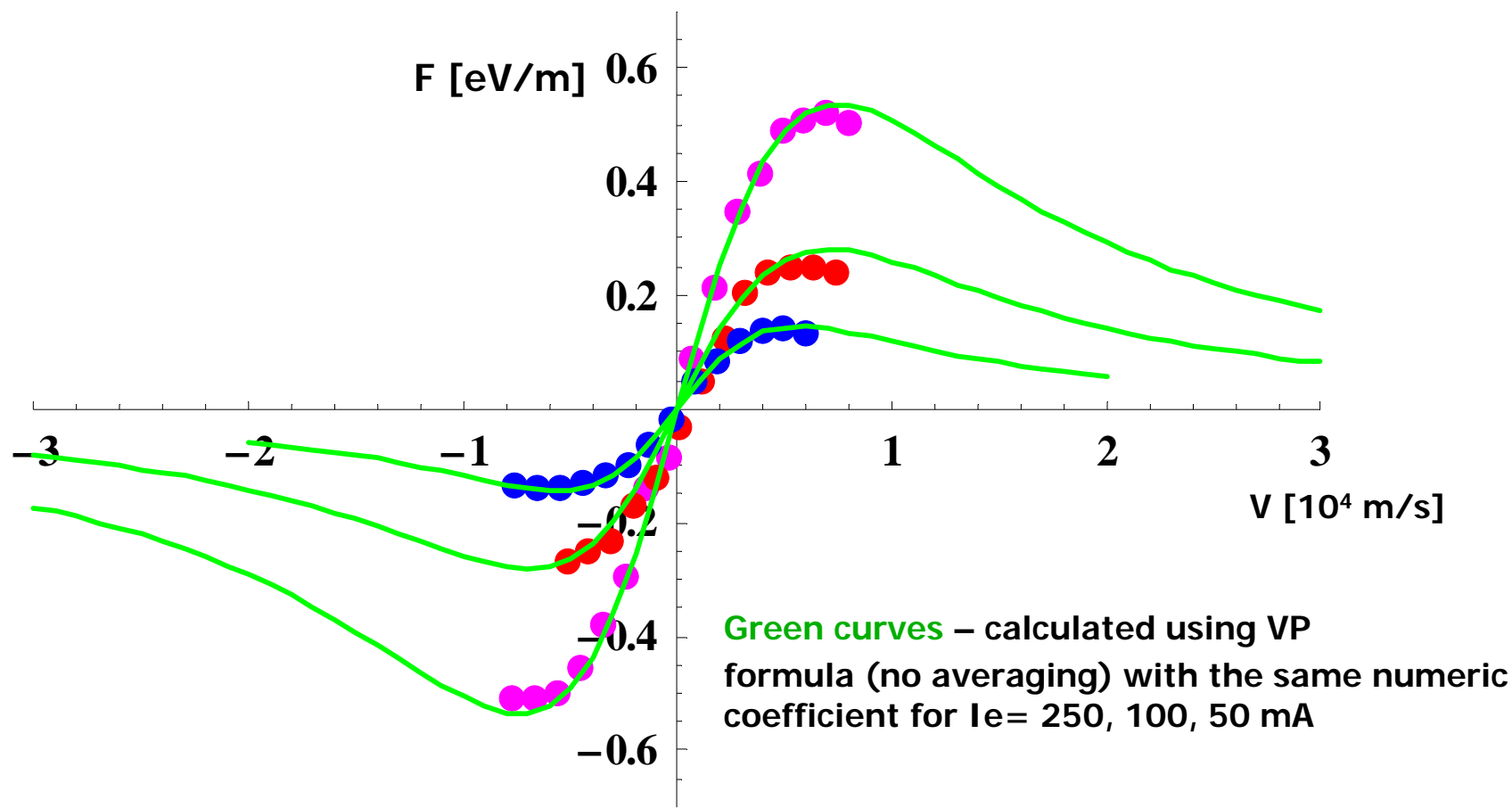
46

empiric formula (VP) – single-particle formula

$$\mathbf{F} = -\frac{1}{\pi} \omega_{pe}^2 \frac{(Ze)^2}{4\pi\epsilon_0} \ln\left(\frac{\rho_{\max} + \rho_{\min} + r_L}{\rho_{\min} + r_L}\right) \frac{\mathbf{V}_{ion}}{(V_{ion}^2 + V_{eff}^2)^{3/2}}$$

March 2 data: $B=0.1\text{T}$, electron current $I_e=250$ (pink color), 100 (red), 50 (blue) mA

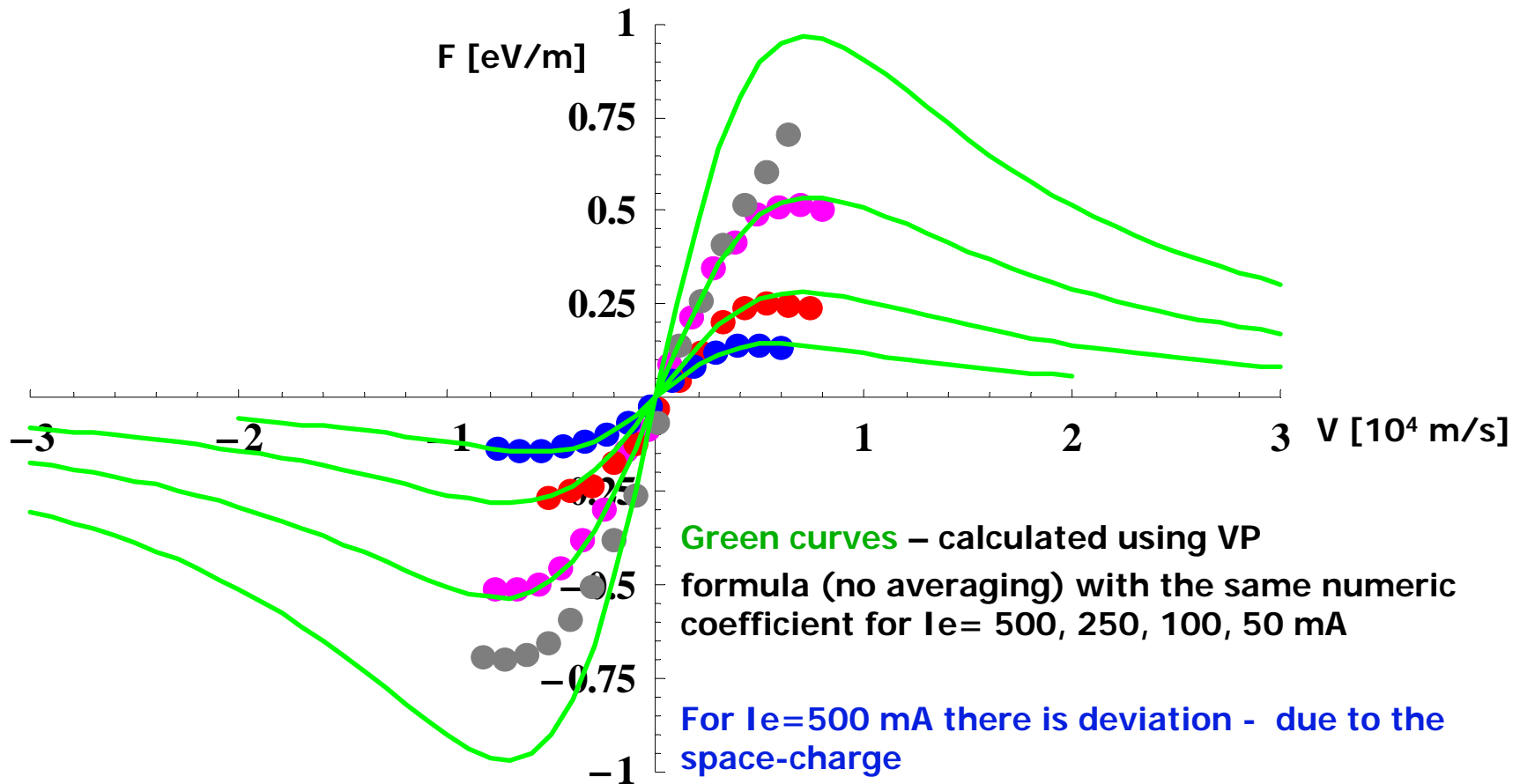
47



March 2 data: $B=0.1\text{T}$

$I_e=500$ (gray), 250 (pink), 100 (red), 50 (blue) mA

48



Electron current $I_e=500\text{mA}$

49

For high currents of the electron beam the space-charge of the electron beam becomes important:

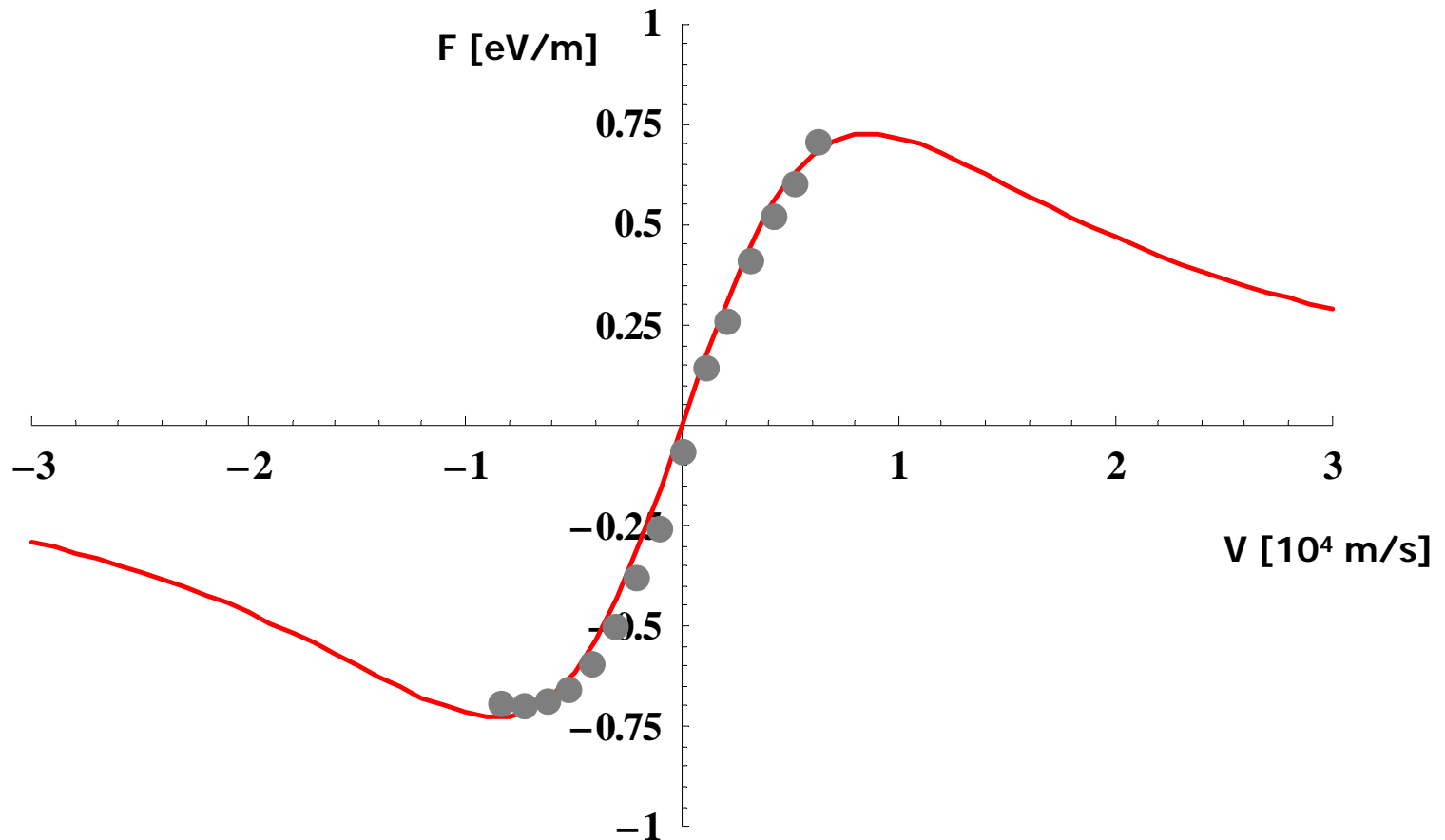
The electron drift in crossed fields – the electric and magnetic fields of the electron beam and longitudinal magnetic field of the cooler:

$$v_d = \frac{2I}{B\beta\gamma^2} \frac{r}{a^2}$$

For measured distribution of the proton beam for the case under comparison (March 2, set#23, $B=0.1\text{T}$, $I_e=500\text{mA}$) - $V_{\text{drift}}=6\text{--}7\cdot 10^3\text{m/s}$ – which is an additional contribution to $V_{\text{effective}}$ in the cooling force formulas.

March 2 data: $I_e=500\text{mA}$, $B=0.1\text{T}$ - formula vs experiment with additional contribution to $V_{\text{effective}}$ from V_{drift}

50



Fits with single-particle formulas

51

1. Current dependence – friction force scales linearly with current/density – as expected from formula.
2. Numeric coefficient for the force is in agreement with the one in Parkhomchuk's formula. Also, it can be adjusted to agree with Derbenev's coefficient (which results in only slightly different effective velocity) – the coefficients are similar for the region of low relative velocities ($1/\pi$ vs $1/(2\pi)^{1/2}$).
3. Note that Coulomb logarithm depends on relative ion velocity and $V_{\text{effective}}$ – fitting was done with such velocity-dependent logarithm.
4. Fitted $V_{\text{effective}}$ has very weak current dependence:

$0.74\text{-}0.78 \cdot 10^4 \text{ m/s}$

Observations

52

- Using single-particle formula allows to fit experimental data and extract $V_{\text{effective}}$.
- However, since rms velocity spreads of cooled proton beam are significant (for our measurements, we would need to have $dp/p=1e-5$ and $\epsilon=1e-9$ m rad to neglect this effect, while parameter of the proton beam with which we did measurements typically had about $dp/p=5e-5$ and $\epsilon=5e-8$ m rad), fitted $V_{\text{effective}}$ has contribution from this effect.

The accurate procedure is then to measure rms velocities of the distribution and average single-particle formulas over the proton distribution.



This was done for all 10's of friction force curves which were measured for various parameters

Detailed comparison: Averaging over ion distribution

53

$$\langle F \rangle = C \frac{4\pi Z^2 e^4 n_e}{m\sqrt{2\pi}\Delta_{\perp}^2 \Delta_{\parallel}} \int_0^{\infty} \int_{-\infty}^{\infty} \frac{v_{\parallel} L_M(v_{\perp}, v_{\parallel}, v_{eff})}{(v_{\perp}^2 + v_{\parallel}^2 + v_{eff}^2)^{3/2}} \exp\left(-\frac{v_{\perp}^2}{2\Delta_{\perp}^2} - \frac{(v_{\parallel} - v_0)^2}{2\Delta_{\parallel}^2}\right) v_{\perp} dv_{\parallel} dv_{\perp}$$

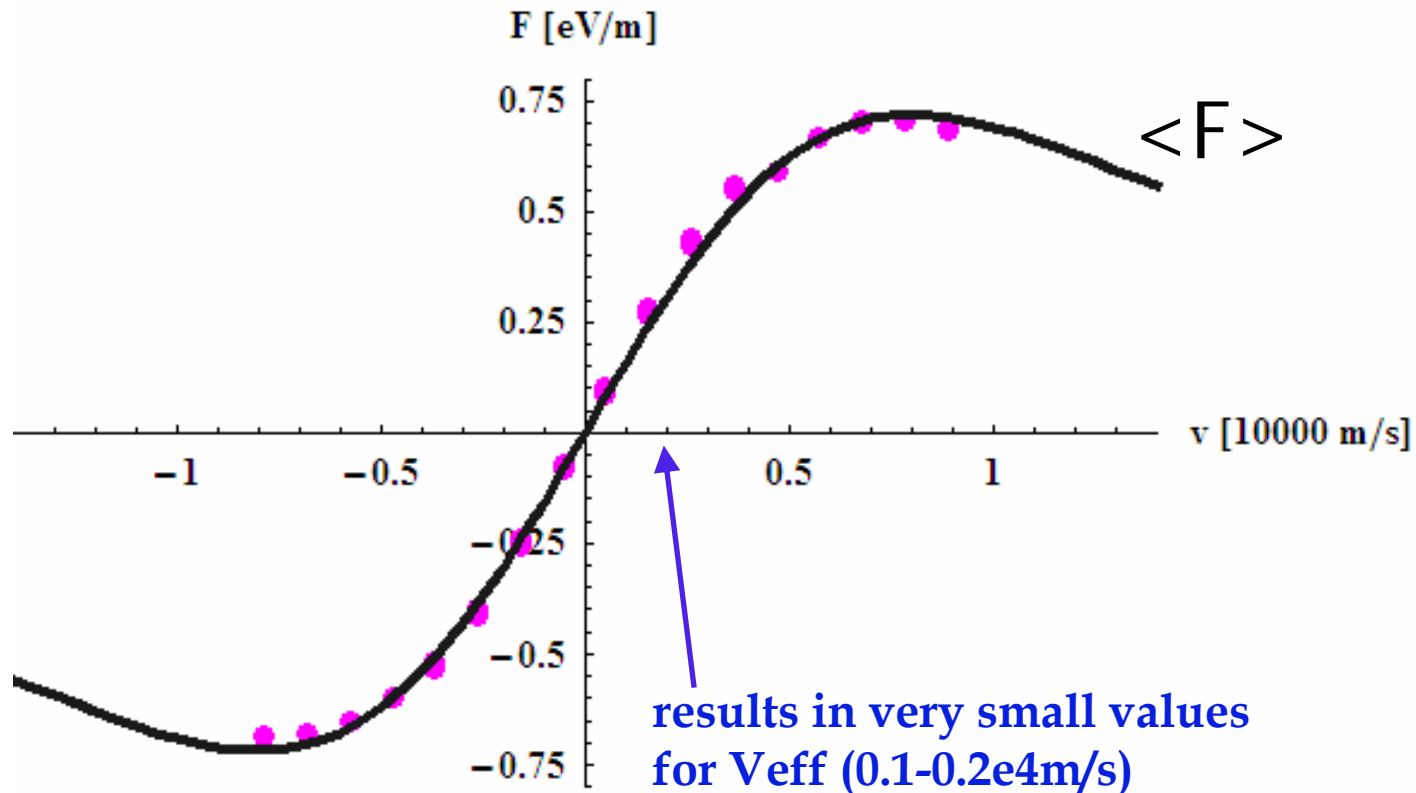
rms parameters of proton beam were measured for each measurement of friction force curve.

1. **First approach:** assume C is known and treat V_{eff} as fitting parameter.
2. **Second approach:** assume V_{eff} is known from measurements and treat C as fitting parameter.

$B=0.12\text{T}$, $I_e=300\text{mA}$

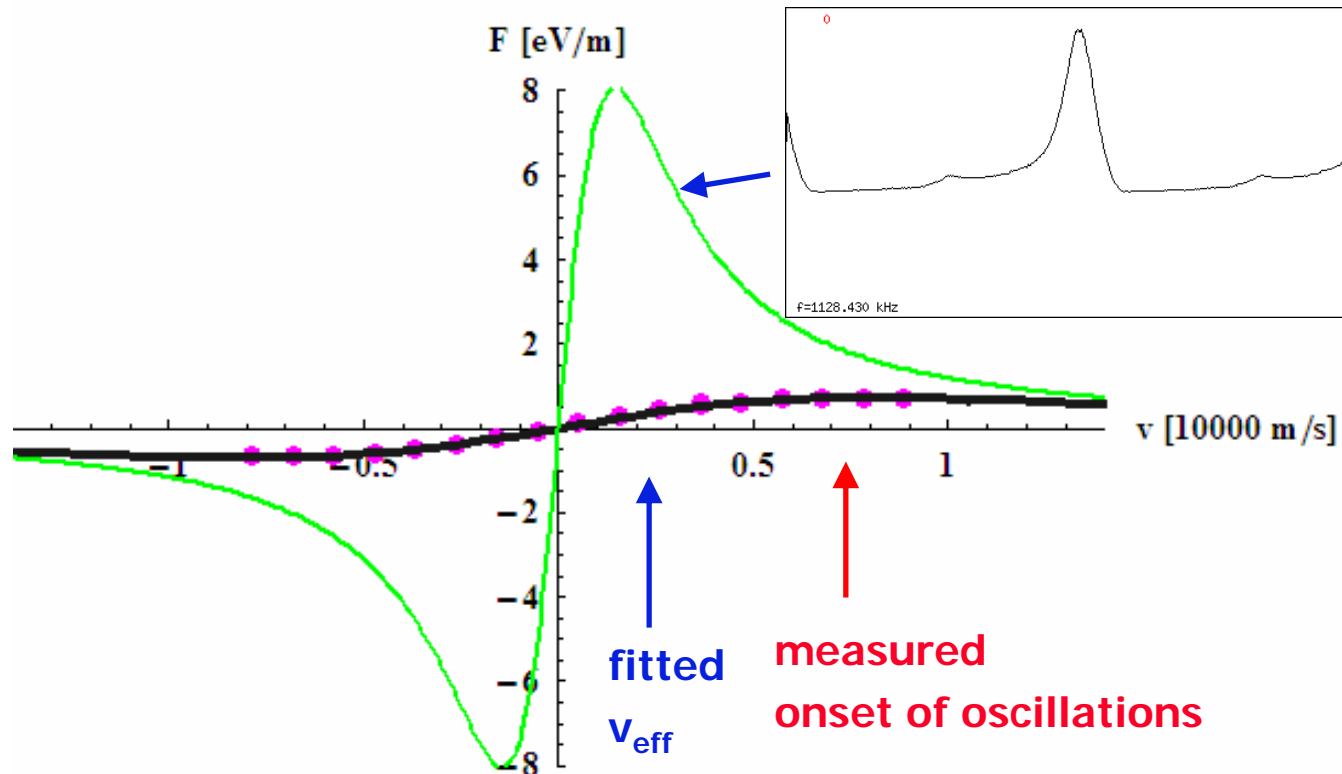
Friction force averaged over proton distribution with measured rms velocity spread

54



First approach – one fitting parameter V_{eff}

55



Longitudinal profiles:
expected
onset of
oscillations
for small v_{eff}

fitted
 v_{eff}

measured
onset of oscillations

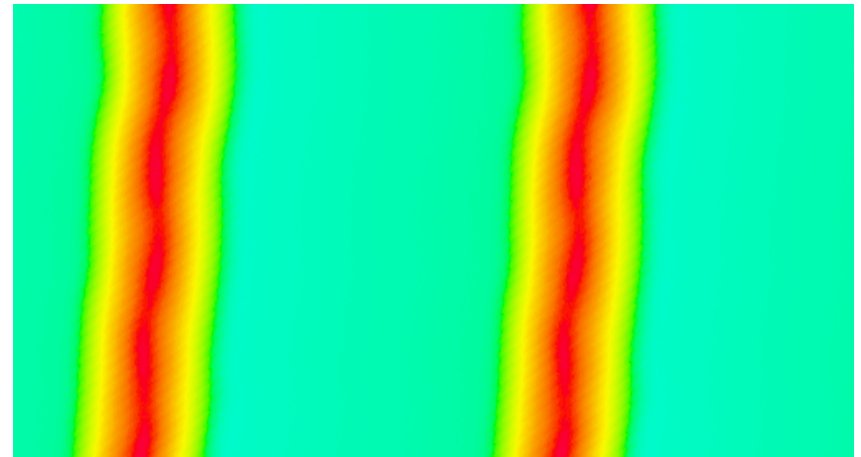
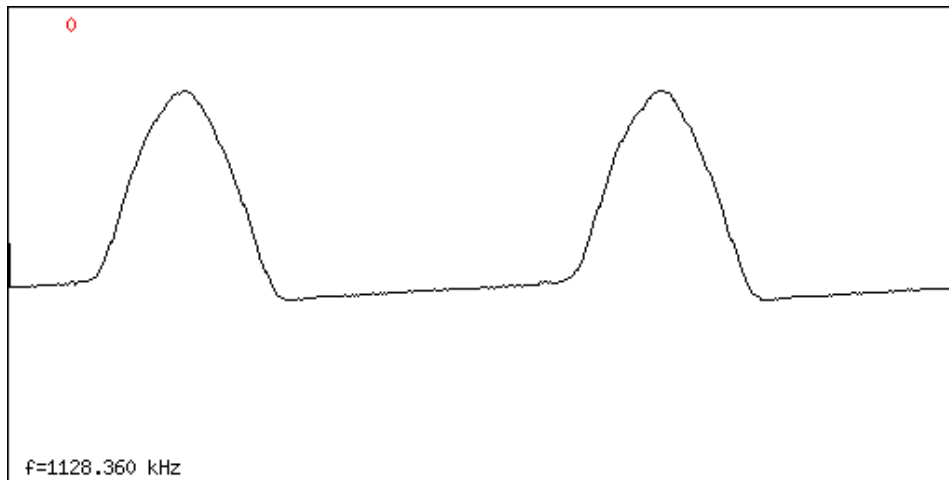
$$\langle F \rangle = C \frac{4\pi Z^2 e^4 n_e}{m\sqrt{2\pi\Delta_\perp^2\Delta_\parallel}} \int_0^\infty \int_{-\infty}^\infty \frac{v_\parallel L_M(v_\perp, v_\parallel, v_{eff})}{(v_\perp^2 + v_\parallel^2 + v_{eff}^2)^{3/2}} \exp\left(-\frac{v_\perp^2}{2\Delta_\perp^2} - \frac{(v_\parallel - v_0)^2}{2\Delta_\parallel^2}\right) v_\perp dv_\parallel dv_\perp$$

$C=1/\pi$

Measurements of longitudinal friction force maximum

56

Approaching friction force maximum

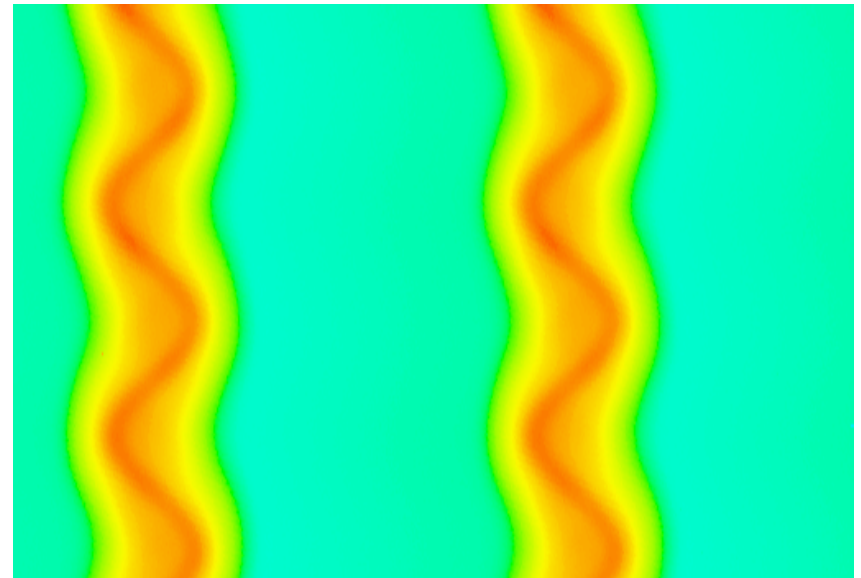
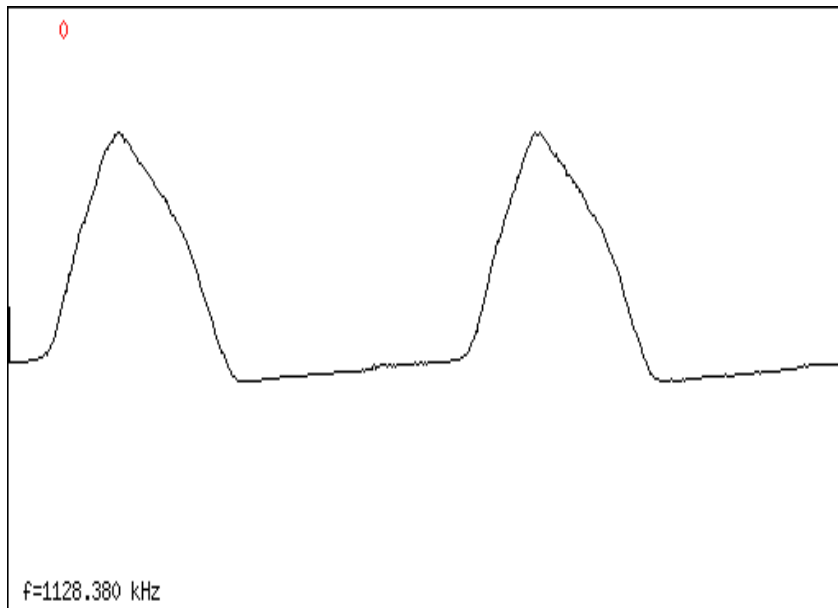


Longitudinal profiles

Measurements of longitudinal friction force maximum

57

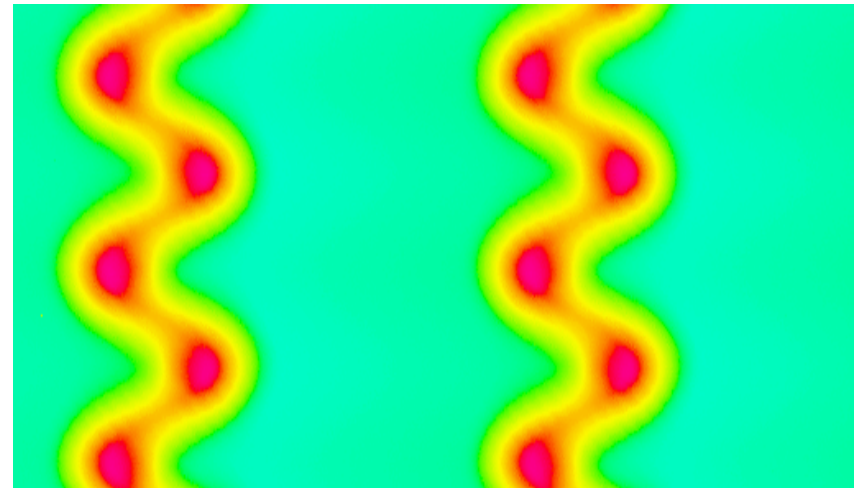
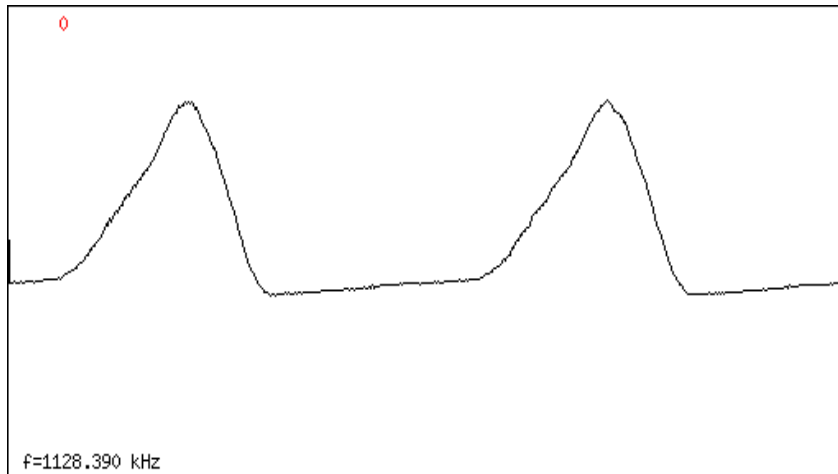
just past the maximum



Measurements in non-linear part of the friction force

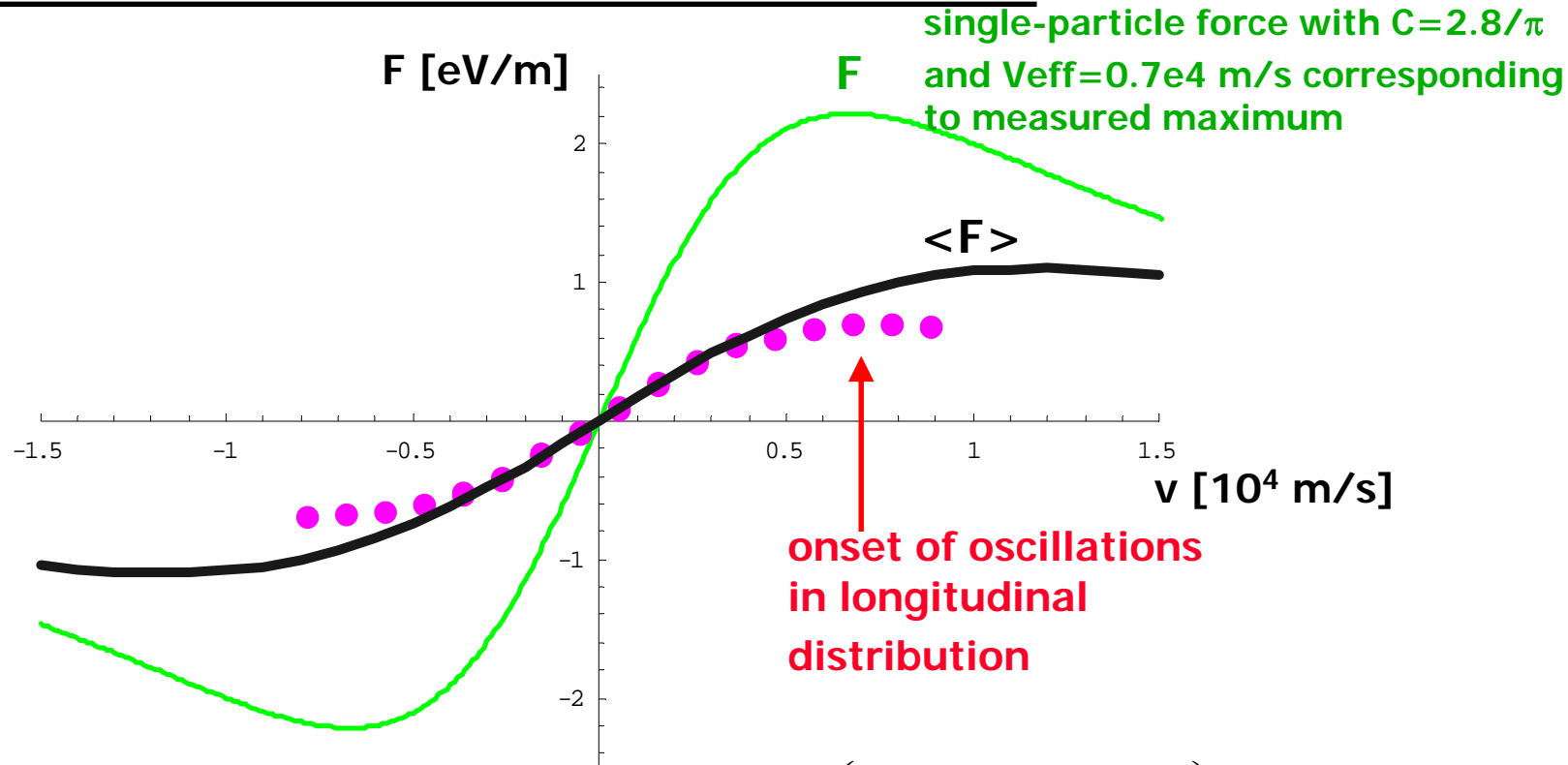
58

far past the maximum



Second approach - one fitting parameter C (with measured V_{eff})

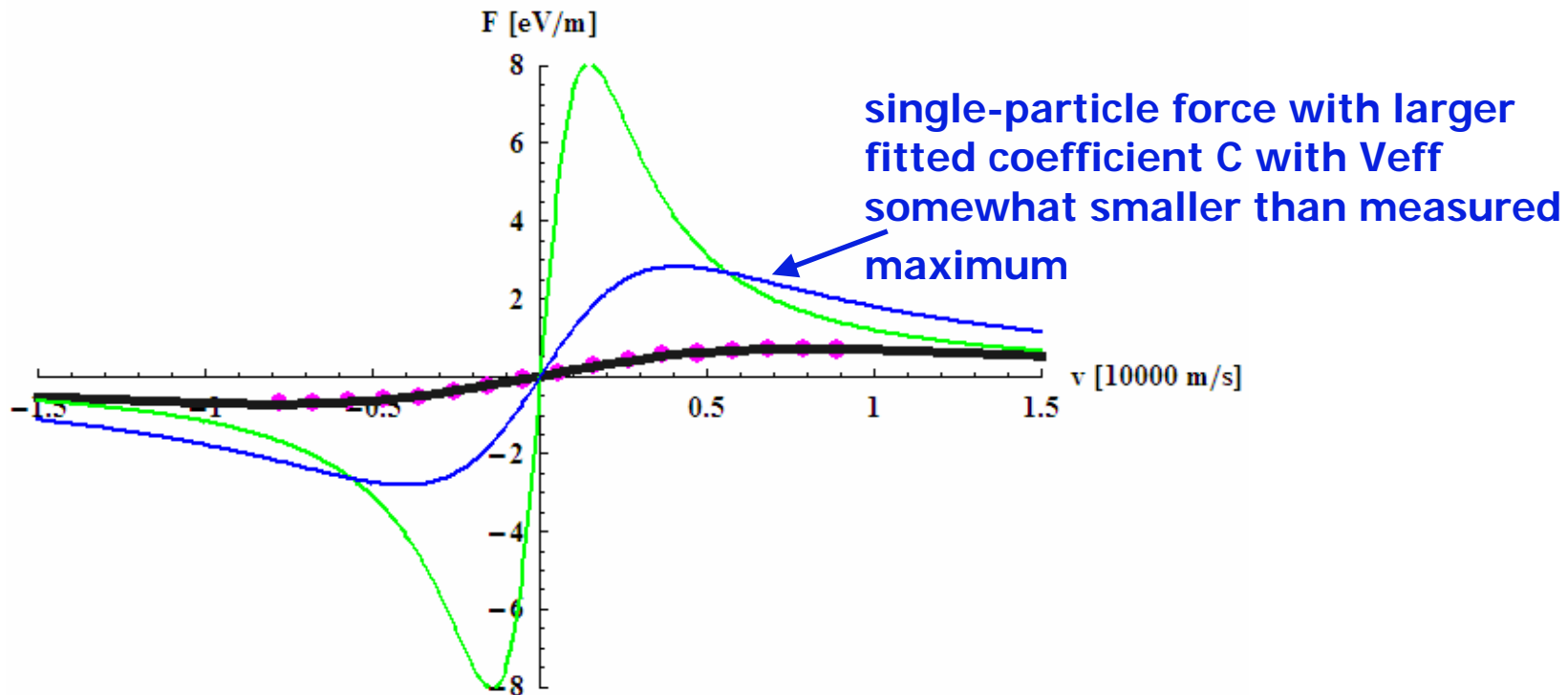
59



$$\langle F \rangle = C \frac{4\pi Z^2 e^4 n_e}{m\sqrt{2\pi}\Delta_{\perp}^2 \Delta_{\parallel}} \int_0^{\infty} \int_{-\infty}^{\infty} \frac{v_{\parallel} L_M(v_{\perp}, v_{\parallel}, v_{eff})}{(v_{\perp}^2 + v_{\parallel}^2 + v_{eff}^2)^{3/2}} \exp\left(-\frac{v_{\perp}^2}{2\Delta_{\perp}^2} - \frac{(v_{\parallel} - v_0)^2}{2\Delta_{\parallel}^2}\right) v_{\perp} dv_{\parallel} dv_{\perp}$$

Second and $1/2$ approach – basically, both C and V_{eff} are fitting parameters (plus averaging)

60



$$\langle F \rangle = C \frac{4\pi Z^2 e^4 n_e}{m\sqrt{2\pi\Delta_\perp^2\Delta_\parallel}} \int_0^\infty \int_{-\infty}^\infty \frac{v_\parallel L_M(v_\perp, v_\parallel, v_{eff})}{(v_\perp^2 + v_\parallel^2 + v_{eff}^2)^{3/2}} \exp\left(-\frac{v_\perp^2}{2\Delta_\perp^2} - \frac{(v_\parallel - v_0)^2}{2\Delta_\parallel^2}\right) v_\perp dv_\parallel dv_\perp$$

Summary – benchmarking of experiments

61

At CELSIUS, we were able to measure longitudinal friction force with very good precision which allows us to use experimental data for accurate benchmarking of theory and simulations.

Parameter dependence of the friction force was measured with “well controlled” condition:

- 1) Current dependence
- 2) Dependence of tilt between electron and proton beams
- 3) Dependence on solenoid errors
- 4) Various degrees of magnetization
- 5) Transient cooling

Benchmarking of experimental data for each of the experiments is presently in progress.

Acknowledgements

62

We would like to thank I. Ben-Zvi, V. Litvinenko, A. Burov, Ya. Derbenev and Electron Cooling Group of RHIC for many useful discussions and help during these studies.

Numerical studies became possible due to support and constant help of Tech-X Corp. with the VORPAL code and Dubna Cooling group with the BETACOOOL code

Experimental studies became possible due to a strong interest expressed by the CELSIUS group. We thank Dag Reistad and The Svedberg Laboratory for providing beam time and support during these experiments. We also thank Oliver Boine-Frankenheim for taking an active role in planning of these experiments.

Thank you for your attention!